

1 **Title:**

2
3 **Exposure to negative socio-emotional events induces sustained**
4 **alteration of resting-state brain networks in older adults**

5
6 **Authors:**

7
8 Sebastian Baez Lugo^{1,2,*}, Yacila I. Deza-Araujo^{1,2}, Christel Maradan², Fabienne Collette³,
9 Natalie L. Marchant⁴, Gaël Chételat⁵, Patrik Vuilleumier^{1,2}, Olga Klimecki^{1,6}, and the Medit-
10 Ageing Research Group

11
12 **Affiliations:**

13
14 ¹ Swiss Center for Affective Sciences, University of Geneva, Geneva, Switzerland.

15 ² Laboratory for Behavioral Neurology and Imaging of Cognition, Department of
16 Neuroscience, Medical School, University of Geneva, Geneva, Switzerland.

17 ³ GIGA-CRC In Vivo Imaging Research Unit, University of Liège, Liège, Belgium.

18 ⁴ Division of Psychiatry, University College London, London, UK

19 ⁵ Université Normandie, Inserm, Université de Caen-Normandie, Inserm UMR-S U1237, GIP
20 Cyceron, Caen, France

21 ⁶ Psychology Department, Technische Universität Dresden, Dresden, Germany.

22
23 * Correspondence concerning this article should be addressed to:
24 **sebastian.baezluogo@unige.ch**

26 **ABSTRACT:**

27

28 Basic emotional functions seem well-preserved in older adults. However, their reactivity to
29 and recovery from socially negative events remain poorly characterized. To address this, we
30 designed a novel "task-rest" paradigm in which 182 participants from two independent
31 experiments underwent functional magnetic resonance imaging while exposed to socio-
32 emotional videos. Experiment 1 (N=55) validated the task in young and older participants and
33 unveiled age-dependent effects on brain activity and connectivity that predominated in resting
34 periods after (rather than during) negative social scenes and related to empathy. Crucially,
35 emotional elicitation potentiated subsequent resting-state connectivity between default mode
36 network (DMN) and amygdala exclusively in older adults. Experiment 2 replicated these
37 results in a large older adult cohort (N=127) and additionally showed that emotion-driven
38 changes in posterior DMN-amygdala connectivity were associated with anxiety, rumination,
39 and negative thoughts. These findings uncover the neural dynamics of empathy-related
40 functions in older adults and help better understand how poor social stress recovery may
41 impact neurodegenerative diseases.

42

43

44

45

46 **Keywords:**

47

48 Aging, Anxiety, Rumination, Default Mode Network, Functional connectivity, Amygdala,
49 Insula, Posterior cingulate cortex, fMRI.

50

51 INTRODUCTION

52
53 Aging is a multifaceted process associated with many changes in bodily and mental health.
54 While there is a general decline in physical performances and cognitive abilities in aging ¹,
55 emotional functions appear to be maintained or even enhanced in older adults relative to
56 younger adults ²⁻⁴. Indeed, the elderly tend to regulate their emotional states well, a crucial
57 capacity for affective well-being and healthy aging ⁵. Unlike younger adults, they often
58 prioritize social and emotional interactions over other goals ⁶ and show a "positivity bias" in
59 emotion perception ⁷. In contrast, maladaptive emotional reactivity and impaired emotion
60 regulation are related to affective psychopathologies such as anxiety, depression, worry, and
61 rumination throughout the lifespan ^{8,9}, including in aging ¹⁰. There is also growing evidence
62 that maladaptive affective styles may represent a significant risk factor for dementia ¹¹⁻¹⁴, one
63 of the primary mental health burdens in the elderly population ¹⁵. However, the neural
64 substrates underpinning proficient socio-affective processing and emotional resilience in the
65 elderly remain unresolved and still scarcely investigated.

66
67 An important marker of maladaptive affective style is "emotional inertia", which
68 denotes the degree to which emotions carry over from one moment to the next ¹⁶. Emotional
69 inertia may reflect unsuccessful recovery mechanisms following the offset of affective events
70 and low resilience to stress, associated with higher risks of depression ^{17,18} and higher trait
71 anxiety and rumination tendencies ¹⁹. Most studies of emotional inertia employed behavioral
72 measures based on experience sampling methods ^{16,20}, e.g., requiring participants to report
73 their affective state at different time points and measuring autocorrelations between
74 successive time-points or events ^{16,21,22}. More recently, a few neuroimaging studies
75 investigated emotional inertia at the brain level using "task-rest" paradigms ²³⁻²⁹. In these
76 studies, brain activity is probed not only during active stimulus processing tasks, but also in
77 spontaneous post-task resting periods during which the brain returns to homeostatic balance
78 ^{30,31}. For example, positive or negative emotions evoked by images or videos were found to
79 induce carryover effects on brain activity and/or connectivity during subsequent resting-state
80 in default mode and affective networks ^{24,28}. These carryover effects have been observed at
81 different time scales ranging from a few seconds ³² to several minutes ²⁷, following different
82 task instructions ranging from passive viewing through to active regulation of emotions ²³,
83 and across different conditions of emotional valence and intensity ^{25,26}.

84

85 At the neural level, most brain imaging studies found carryover effects of emotions on
86 the functional dynamics of the default mode network (DMN) either in the form of increased
87 ^{26,32} or decreased ^{24,25} activity patterns in regions comprising the medial prefrontal cortex
88 (MPFC), posterior cingulate cortex (PCC), precuneus, and inferior parietal cortex. These
89 regions of the DMN are usually active when individuals are free to let their mind wander in
90 undisturbed conditions ^{33,34}. Similar effects have also been observed in the insula and
91 amygdala ²⁴; two regions critically involved in emotional and social processing ^{35–37}. For
92 instance, a slow recovery of amygdala activity (i.e., longer return to baseline level) after
93 negative images was reported in individuals with higher neuroticism ³⁸. Slower recovery of
94 amygdala activity after emotional videos was furthermore associated with higher anxiety
95 traits and ruminations ¹⁹. Subcortical limbic regions such as the amygdala and striatum also
96 display sustained changes in their functional connectivity with cortical areas in medial PFC
97 and PCC during rest after negative emotions ²⁴ and reward ²⁸. These findings converge with
98 studies showing that disturbances in functional connectivity of the amygdala with medial
99 parts of the DMN at rest are associated with anxiety (e.g., decreased connectivity with MPFC
100 ³⁹) and mood disorders (e.g., increased connectivity with PCC ⁴⁰). Taken together, these data
101 suggest that long-lasting carryover effects of emotions on activity and connectivity of limbic
102 networks may provide an important neural marker of emotional regulation style and affective
103 resilience.

104

105 However, all previous neuroimaging studies of emotional carryover focused on young
106 healthy participants. It remains unknown whether emotional inertia also occurs in older
107 adults, how it is modified given the well-known “positivity bias” observed in this population
108 ^{2,3}, and how age impacts the functional dynamics of DMN in affective contexts. Indeed, it has
109 been reported that, unlike young adults, older people fail to deactivate the DMN during
110 externally directed cognitive tasks ⁴¹ and show increased DMN connectivity with cognitive-
111 related prefrontal regions ⁴². Yet, little is known about how aging affects DMN interaction
112 with emotion-related regions, either during or after emotional tasks, and how it relates to other
113 cognitive or socio-affective abilities.

114

115 In addition, previous work did not assess whether emotional inertia is modulated by
116 individual differences in empathy, which may strongly influence how people react to negative
117 socio-affective stimuli presented in neuroimaging studies ^{19,24}, and thus how they recover
118 from induced emotions ²⁷. Because social competencies and affective empathy are relatively

119 preserved in the elderly ⁴, socially significant emotional events offer an optimal window to
120 probe emotional reactivity and recovery in this population. Moreover, there is only scarce
121 research on empathy in older people ^{4,43-47}. Whereas cognitive empathy may decline in older
122 compared to younger people, affective empathy and altruistic behaviors towards others
123 remain intact or even improve ^{4,47-49}. However, brain responses to seeing others' pain are
124 reduced in anterior insula (AI) and cingulate cortex (ACC) ⁴³, two regions implicated in pain
125 processing, negative affect, and salience detection ^{36,50}. In contrast, empathy-related responses
126 may increase in superior temporal sulcus (STS) and temporo-parietal junction (TPJ) ⁴⁶, brain
127 regions frequently associated with Theory of Mind and perspective taking ⁵¹. Yet, despite the
128 importance of social interactions and emotional resilience for healthy aging ⁵²⁻⁵⁴, neural
129 substrates underlying the recovery from negative events, as well as their link with empathic
130 skills, personality and psycho-affective traits, have not been investigated during aging.

131

132 To address these issues, we designed a novel "task-rest" paradigm combining two
133 lines of research: short (10-18s) empathy inducing videos from the Socio-affective Video
134 Task (SoVT) ⁵⁵ were shown interspersed with rest periods of 90 seconds (similar to Eryilmaz
135 and colleagues ²⁴) while participants underwent functional magnetic resonance imaging
136 (fMRI) of brain activity. The SoVT videos consisted of short silent scenes depicting suffering
137 people (high emotion videos) or people in everyday life situations (low emotion videos). By
138 adding short resting-state periods after blocks of videos of each kind, the SoVT-Rest allowed
139 us to evaluate how the aging brain reacts both during and after exposure to emotionally
140 challenging social information. Indeed, defining valid markers of adaptive emotion recovery
141 abilities in a naturalistic paradigm, without making high cognitive demands required by more
142 voluntary/explicit regulation strategies ⁵⁶, would be valuable to better understand affective
143 resilience mechanisms and better predict affective risk factors associated with pathological
144 aging and dementia ¹⁴.

145

146 Here, we use the new SoVT-Rest paradigm across two independent experiments to
147 probe for emotion-related carryover effects in large samples of healthy older and young
148 participants. First, we test for differences in the neural substrates of emotional recovery
149 between old and young (Experiment 1), allowing us to validate our paradigm, verify relevant
150 neural effects and assess the effect of age. Next (Experiment 2), we replicate this experiment
151 in a large sample of elderly participants (n=127) in whom we specifically asked whether
152 emotional inertia in brain networks is modulated by empathy and individual traits relevant for

153 healthy aging, including rumination and anxiety. We hypothesized that exposure to others'
154 suffering (relative to neutral social situations) should (1) engage brain regions implicated in
155 emotional saliency and empathy (i.e., insula, aMCC), but with lower responses in older than
156 young adults ⁴³; (2) induce subsequent carryover in functional connectivity at rest between
157 emotion-related regions and the DMN, with differential age-dependent patterns; and (3)
158 unveil neural substrates of emotional inertia that may reflect individual variability in anxiety,
159 ruminative thinking, and negative emotions, and thus point to functional biomarkers of
160 affective risk factors for pathological aging ¹¹⁻¹⁴. In addition, (4) we should observe a
161 “positivity effect” as often reported in older adults ⁷ and elucidate its relationship to empathy
162 processes during aging.

163

164 MATERIAL AND METHODS

165

166 Participants

167 For Experiment 1, a total of 58 healthy participants including 30 younger adults (aged
168 between 19 and 30 years), and 28 older adults (aged between 65 and 78 years) with corrected-
169 to-normal vision, no history of neurological, psychiatric disorder, or alexithymia took part.
170 Thirty participants were expected to participate in each group; however, new research
171 guidelines during the COVID-19 pandemic prevented us from continuing with scanning.
172 Recruitment was performed through social media and advertisement in various locations
173 within the University of Geneva. Three participants were excluded due to a priori exclusion
174 criteria including artifacts in brain images and/or extreme head motion during scanning. The
175 final sample for Experiment 1 included 29 young participants (*M* age= 24, 14 females) and 26
176 older participants (*M* age = 68.7, 13 females), resulting in a total of N=55 participants (See
177 Table 1 for detailed participants' characteristics). All participants provided written informed
178 consent. This study was approved by the local Swiss ethics committee (commission cantonale
179 d'éthique de la recherche CCRE, Geneva) under the project number 2018-01980.

180

181 For Experiment 2, a total of 135 healthy older adults participated, with corrected-to-normal
182 vision and no history of neurological or psychiatric disorders, aged between 65 and 83 years.
183 This session was part of the baseline visit of the Age-Well randomized clinical trial within the
184 Medit-Ageing Project ⁵⁷, conducted in Caen (France). Detailed inclusion criteria of the Age-
185 Well randomized clinical trial are provided in Supplementary Table 1. Participants were

186 recruited via advertising in media outlets, social media, and flyers distributed in relevant local
187 events and locations. A total of 8 participants were excluded from the final data analysis due
188 to a priori exclusion criteria: abnormal brain morphology ($n = 3$), extreme head motion ($n =$
189 3), and presence of artifacts in brain images ($n = 2$). The final sample for this study included
190 127 participants (M age = 68.8 years, $SD = 3.63$, 79 females. See Table 1 for other
191 characteristics). All participants provided written informed consent prior to participation. The
192 Age-Well randomized clinical trial was approved by the ethics committee (Comité de
193 Protection des Personnes Nord-Ouest III, Caen, France; trial registration number: EudraCT:
194 2016-002441-36; IDRCB: 2016-A01767-44; ClinicalTrials.gov Identifier: NCT02977819).

195

196 **Questionnaires**

197 In order to account for inter-individual differences in psycho-emotional profile, all
198 participants from both experiments answered several questionnaires assessing psycho-
199 affective traits and cognitive functions, including empathy (Interpersonal Reactivity Index,
200 IRI⁵⁸), depression (Geriatric Depression Score, GDS⁵⁹ for older adults and Beck Depression
201 Inventory, BDI⁶⁰ for younger adults), anxiety (STAI-trait Anxiety Index, STAI⁶¹), emotion
202 regulation capacities (Emotion Regulation Questionnaire, ERQ⁶²), and rumination levels
203 (Rumination Response Scale, RRS⁶³). A summary of these questionnaires is provided in
204 Table 1 and Fig. 3. All scores were in the normative range. For a full list of tasks and
205 measures in the Age-Well trial (Experiment 2), please refer to Poisnel and colleagues⁵⁷.

206

207

TABLE 1. Participant characteristics

		Experiment 1		<i>P</i> value for between-group differences ^a	Experiment 2
		Mean (SD)			Mean (SD)
		N=55			N=127
		YA Group (n = 29)	OA Group (n = 26)		OA Group
<i>Demographics</i>					
Sex		14 Females	13 Females		79 Females
Age		24.5 (2.67)	68.7 (3.89)		68.8(3.65)
Education (n. of years)		18.4 (1.72)	16.1 (3.4)	0.002	13.21 (3.1)
<i>Psycho-affective traits and Cognitive functions</i>					
STAI	Trait	39.8 (8.31)	36(7.31)	0.08	34.57 (7.12)
Rumination Response Scale^b	Total	43.5 (10)	36.5 (9.01)	0.008	35.67 (8.55)
	Reflection	11.3 (3.67)	8.77 (3.52)	0.01	8.93 (3.23)
	Brooding	8.97 (2.64)	8.69 (2.41)	0.69	8.06 (2.28)
Interpersonal Reactivity Index	Distress	12 (4.3)	9.62 (5.12)	0.07	10.18 (5.27)
	Empathic Concern	22.1 (3.14)	20.8 (4.24)	0.19	19.76 (4.18)
	Perspective Taking	21.3 (3.71)	17.3 (3.42)	<0.001	17.50 (3.56)
	Fantasy	19.1(4.05)	15.8 (4.08)	0.004	14.35 (4.75)
Emotion regulation abilities	Reappraisal	30.5 (7.11)	29.2 (3.95)	0.4	29.61 (5.79)
	Suppression	12.6 (5.48)	14.8 (4.34)	0.09	16.54 (5.19)
Beck Depression Inventory	Global	5.34 (3.73)			
Geriatric Depression Scale	Global	1.92 (2.3)			1.32 (1.78)

Abbreviations: YA, younger adults; OA, older adults; N, number of total participants in each experiment; n, number of participants in each subgroup; SD, Standard deviation. ^aBetween-group differences were assessed using *t*-tests, statistical significance was set to $P < .05$. ^b Values computed on n=126 participants (data missing for one participant).

208

209

210 Socio-affective Video Task-Rest (SoVT-Rest)

211

212 The emotion-elicitation task used in both experiments was adapted from the previously

213 validated Socio-affective Video Task (SoVT)^{55,64}. The SoVT aims to assess social emotions

214 (e.g., empathy) in response to short silent videos (10-18s). During this task, participants watch

215 12 High Emotion (HE) and 12 Low Emotion (LE) video clips grouped in blocks of three (see

216 instructions in supplementary Table 2). HE videos depict people suffering (e.g., due to

217 injuries or natural disasters), while LE videos depict people during everyday activities (e.g.,

218 walking or talking). In this study, each block was followed by a resting state period of 90

219 seconds (see instructions in Fig. 1 and supplementary Table 2) in order to assess the carryover

220 effects of emotion elicitation on subsequent resting-state brain activity (similar to Eryilmaz

221 and colleagues²⁴). This combination of both paradigms (task and rest) was specifically

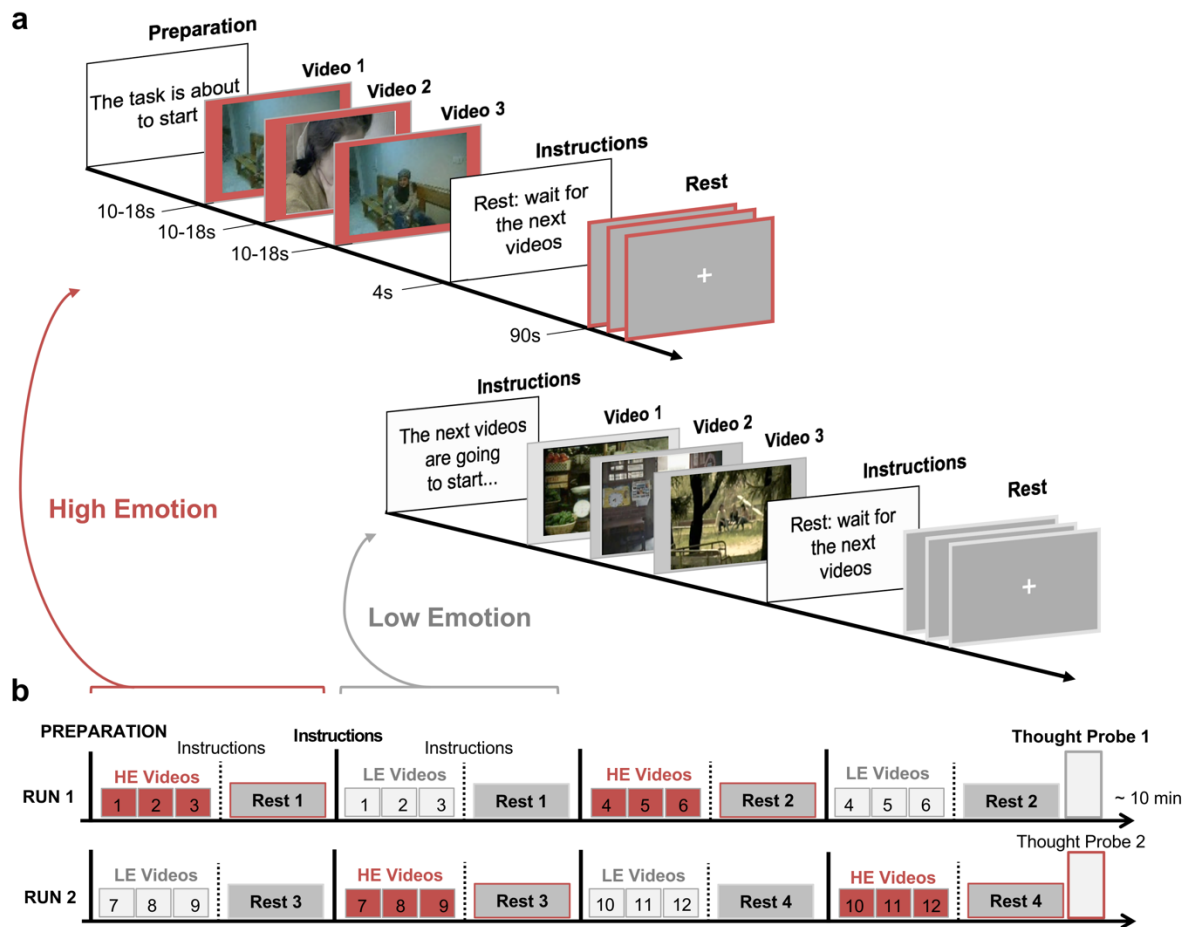
222 designed to test for emotional inertia and its relation to empathy. The combined task (SoVT-

223 Rest) is illustrated in Fig. 1.

224 Overall, three sets (V1, V2, and V3) of 24 videos each were created and randomized
225 across participants. In Experiment 1, the video sets V1, V2, and V3 were seen by $n = 21$, 18,
226 and 16 participants, respectively. In Experiment 2, these were seen by $n = 42$, 40, and 45
227 participants, respectively. During the SoVT-Rest, these videos were presented in two separate
228 runs, with each run followed by a thought probe to assess current mental content during the
229 last rest period (after LE videos in one run and after HE videos in the other run). The order in
230 which runs were presented was randomized so that half of the participants started the
231 experiment with a HE block and the other half with an LE block. The total duration of the
232 SoVT-Rest fMRI paradigm was approximately 21 minutes, consisting of 9.5 min for each run
233 plus 1 minute on average for each thought probe.

234 After the fMRI session, participants watched all video clips again on a computer
235 outside the scanner and provided ratings on their subjective experience of empathy (“To what
236 degree did you feel the emotions of the characters?”) as well as their subjective positive affect
237 (“Indicate the intensity of your positive emotions”) and negative affect state (“Indicate the
238 intensity of your negative emotions”) (translated from French), for each of the 24 videos.
239 Each scale offered 21 possible responses ranging from 0 (“Not at all”) to 10 (“Extremely”)
240 with increments of 0.5. The order of questions was always the same: empathy, positive affect,
241 and negative affect. We chose to obtain ratings after fMRI not only to minimize the time older
242 adults spent in the scanner, but also to avoid potential cognitive effects during scanning that
243 may confound neural activity during emotional perception and spontaneous rest recovery
244 periods^{65,66}. The total time for post-scanning ratings was, on average, 10 minutes. Onset times
245 and response times for both neuroimaging and behavioral tasks were collected via the Cogent
246 toolbox (developed by Cogent 2000 and Cogent Graphics) implemented in Matlab 2012
247 (Mathworks Inc., Natick, MA, USA).

248
249



250

251

252 **Figure 1. Experimental design:** (a) SoVT-Rest paradigm: 12 **High Emotion (HE)** and 12 **Low Emotion (LE)**
 253 videos were presented grouped in blocks of three. HE videos depict suffering people (e.g., due to injuries or
 254 natural disasters), while LE videos depict people during everyday activities (e.g., walking or talking). Each block
 255 of three videos is followed by a resting state period of 90 seconds. (b) Each run ends with a thought probe in
 256 which participants verbally express what they had been thinking and/or feeling during the last rest period (via a
 257 microphone), once following a LE block and once following a HE block. The order of the runs was randomized
 258 between participants.

259

260 Behavioral data analysis.

261 We performed a repeated measure multivariate analysis of variance (MANOVA, with Pillai's
 262 trace statistics) with the within-subject factor “video type” (HE and LE), the between-subject
 263 factor “video set” (V1, V2, V3), and three dependent variables: ratings of empathy, positive
 264 affect, and negative affect. This was followed up by pairwise *t*-tests. We also computed
 265 Spearman’s rank correlations between these different scores. Additionally, we performed
 266 correlation analyses between ratings of empathy, positive affect, and negative affect of videos
 267 and age (as a continuous variable), using non-parametric Spearman’s rank correlations
 268 because some of these variables were not normally distributed. All statistical analyses are
 269 reported with a significance level of $P < 0.05$, and when necessary, P values are corrected for

270 multiple comparisons using the False Discovery Rate (FDR) method ⁶⁷. The statistical
271 analyses were performed with R studio (version 3.6.1) and the corresponding graphs were
272 created with ggplot2 (version 3.2.1).

273

274 **Acquisition and preprocessing of MRI data.**

275

276 **Experiment 1**

277

278 Magnetic Resonance Imaging (MRI) scans were acquired at the Brain and Behavior
279 Laboratory of the University of Geneva, using a 3T whole-body MRI scanner (Trio TIM,
280 Siemens, Germany) with the 32-channel head coil. A high-resolution T1-weighted anatomical
281 volume was first acquired using a magnetization-prepared rapid acquisition gradient echo
282 (MPRAGE) sequence (repetition time = 1900 ms; echo time = 2.27 ms; flip angle = 9°; slice
283 thickness = 1 mm; field of view = 256x256 mm²; in plane resolution = 1x1 mm²). Blood
284 oxygen level-dependent (BOLD) images were acquired with a susceptibility weighted EPI
285 sequence (TR/TE = 2000/30 ms, flip angle = 85°, voxel size (3 x 3 mm), 35 slices, 3 mm slice
286 thickness, 20% slice gap, direction of acquisition = descending). Quality control and
287 preprocessing were conducted using Statistical Parametric Mapping software (SPM12;
288 Wellcome Trust Centre for Neuroimaging, London, United Kingdom) on Matlab 2017
289 (Mathworks Inc., Natick, MA, USA). Prior to preprocessing, we manually centered all images
290 to the AC-PC axis, aligned the functional and anatomical MRI images, and then realigned all
291 images to the SPM anatomical template. Preprocessing included the following steps: 1) EPI
292 data were realigned to the first volume and spatially smoothed with an 8-mm FWHM
293 Gaussian kernel. 2) Preprocessed fMRI data were denoised for secondary head motion and
294 CSF-related artifacts using automatic noise selection as implemented in ICA-AROMA, a
295 method for distinguishing noise-related components based on ICA decomposition ⁶⁸.
296 Additionally, components with high spatial overlap with white matter regions were also
297 removed by means of a linear regression using the `fsl_regfilt` function of FSL (FMRIB's
298 Software Library, www.fmrib.ox.ac.uk/fsl). 3) Denoised EPI data were coregistered to the
299 anatomical T1 volume. 4) The anatomical T1 volume was segmented and the extracted
300 parameters were used to 5) normalize all EPIs volumes into the Montreal Neurological
301 Institute (MNI) space. This procedure was performed using FSL and SPM12.

302

303

304 **Experiment 2**

305

306 Magnetic Resonance Imaging (MRI) scans were acquired at the GIP Cyceron (Caen, France)
307 using a Philips Achieva (Eindhoven, The Netherlands) 3T scanner with a 32-channel head
308 coil. Participants were provided with earplugs to protect hearing, and their heads were
309 stabilized with foam pads to minimize head motion. A high-resolution T1-weighted
310 anatomical volume was first acquired using a 3D fast field echo sequence (3D-T1-FFE
311 sagittal; repetition time = 7.1 ms; echo time = 3.3 ms; flip angle = 6°; 180 slices with no gap;
312 slice thickness = 1 mm; field of view = 256x256 mm²; in plane resolution = 1x1 mm²). Blood
313 oxygen level-dependent (BOLD) images were acquired during the SoVT-Rest task with a
314 T2*-weighted asymmetric spin-echo echo-planar sequence (each run ~10.5 min; TR = 2000
315 ms, TE = 30 ms, flip angle = 85°, FOV = 240 x 240 mm², matrix size = 80 x 68 x 33, voxel
316 size = 3 × 3 × 3 mm³, slice gap = 0.6 mm) in the axial plane parallel to the anterior-posterior
317 commissure. During each functional run, about 310 contiguous axial images were acquired
318 and the first two images were discarded because of saturation effects. Additionally, in order to
319 improve the preprocessing and enhance the quality of the BOLD images ⁶⁹, T2 and T2*
320 structural volumes were collected. Each functional and anatomical image was visually
321 inspected to discard susceptibility artifacts and anatomical abnormalities.

322 Quality control and preprocessing were conducted using Statistical Parametric
323 Mapping software (SPM12; Wellcome Trust Centre for Neuroimaging, London, United
324 Kingdom) on Matlab 2017 (Mathworks Inc., Natick, MA, USA). Prior to the preprocessing,
325 we manually centered the images to the AC-PC axis, realigned the functional and anatomical
326 MRI images and then realigned all images to the last version of the SPM anatomical template.
327 The preprocessing procedure was done with SPM12 and followed a methodology designed to
328 reduce geometric distortion effects induced by the magnetic field, described by Villain and
329 colleagues ⁶⁹. This procedure included the following steps: 1) realignment of the EPI volumes
330 to the first volume and creation of the mean EPI volume, 2) coregistration of the mean EPI
331 volume and anatomical T1, T2, and T2* volumes, 3) warping of the mean EPI volume to
332 match the anatomical T2* volume, and application of the deformation parameters to all the
333 EPI volumes, 4) segmentation of the anatomical T1 volume, 5) normalization of all the EPIs,
334 T1 and T2* volumes into the Montreal Neurological Institute (MNI) space using the
335 parameters obtained during the T1 segmentation, 6) 8 mm FWHM smoothing of the EPI
336 volumes.

337 For each individual, frame-wise displacement (FD) ⁷⁰ was calculated. FD values
338 greater than 0.5 mm were flagged to be temporally censored or “scrubbed” during the first-
339 level analysis (see description below). The average of FD volumes censored was $M = 6.8$ (SD
340 $= 8.3$, $Min = 1$, $Max = 38$) for both runs for a total of $n=65$ participants. Three participants
341 were excluded from further analysis because $>10\%$ of volumes a $FD > 0.5$ mm within one
342 run.

343

344 **General linear model analysis with SPM**

345 For both experiments, the MRI SoVT-Rest data was analyzed using General Linear Models in
346 SPM12 (implemented in Matlab 2017). This comprised standard first-level analyses at the
347 subject level, followed by random effect (2nd-level) analyses to assess the effects of interest
348 at the group level. For the 1st-level analysis, a design matrix consisting of two separate
349 sessions was constructed for each participant. Experimental event regressors in each session
350 included the fixation cross (10 sec), instructions (8 sec in Experiment 1, 4 sec in Experiment
351 2), the three videos (~15 sec each) modeled separately, and the rest periods following each
352 block (90 sec). Each rest period was divided into three equal parts (30 sec time bins) in order
353 to model different time intervals during which brain activity may gradually change after the
354 end of the HE and LE video blocks (similar to Eryilmaz and colleagues ²⁴).

355 The different regressors were then convolved with a hemodynamic response function
356 (HRF) according to a block design for univariate regression analysis. The six realignment
357 parameters were added to the matrices in order to account for motion confounds, and low-
358 frequency drifts were removed via a high-pass filter (cutoff frequency at $1/256$ Hz). The
359 final 1st-level matrix consisted of 2 sessions of 21 regressors each (1 fixation cross + 1
360 instruction for videos + 1 instructions for rest + 3 HE videos + 3 post HE rest + 3 LE videos +
361 3 post LE rest + 6 motion parameters). Additionally, we addressed the influence of remaining
362 motion on BOLD data by performing data censoring as described by Power and colleagues ⁷⁰.
363 Specifically, during the estimation of beta coefficients for each regressor of interest, volumes
364 with $FD > 0.5$ mm were flagged in the design matrices and ignored during the estimation of
365 the 1st-levels.

366 For the 2nd-level analyses, we used flexible factorial designs where the estimated
367 parameters from 1st-level contrasts of interest were entered separately for each subject. The
368 second-level design matrix was generated with SPM12 and included 12 regressors of interest
369 (3 HE videos + 3 Post HE rest + 3 LE videos + 3 Post LE rest). This step allowed us to

370 investigate the effect of each experimental condition on brain activity, including the main
371 condition effects (video and rest), the specific emotional effects (HE and LE) during either the
372 video or the subsequent rest periods as well as the age effect on the different conditions
373 (young vs. old, Experiment 1).

374 In both experiments, we conducted *t*-tests contrasts to compare the conditions of
375 interest (videos vs. rest periods and vice versa) and the specific emotional effects (videos: HE
376 vs. LE; rest: HE vs. LE). In Experiment 1, we additionally tested for age differences in these
377 effects (OA vs. YA (videos: HE vs. LE); OA vs. YA (rest: HE vs. LE)). In Experiment 1,
378 results are reported at *P* uncorrected < 0.001, *k* > 20 which has been shown to be acceptable
379 and reliable for fMRI experiments assessing cognitive and affective processes with unprecise
380 onsets ⁷¹, and clusters surviving whole-brain family-wise error correction at *P* < 0.05 at the
381 cluster level (FWEc) are indicated in figures and tables (see supplementary Table 3a). In
382 Experiment 2, all comparisons are reported with a whole-brain FWE correction at *P* < 0.05, at
383 the voxel level (see supplementary Table 3b).

384

385 **Functional connectivity analysis during rest periods, definition of Regions of** 386 **Interest (ROI), and the data analysis pipeline**

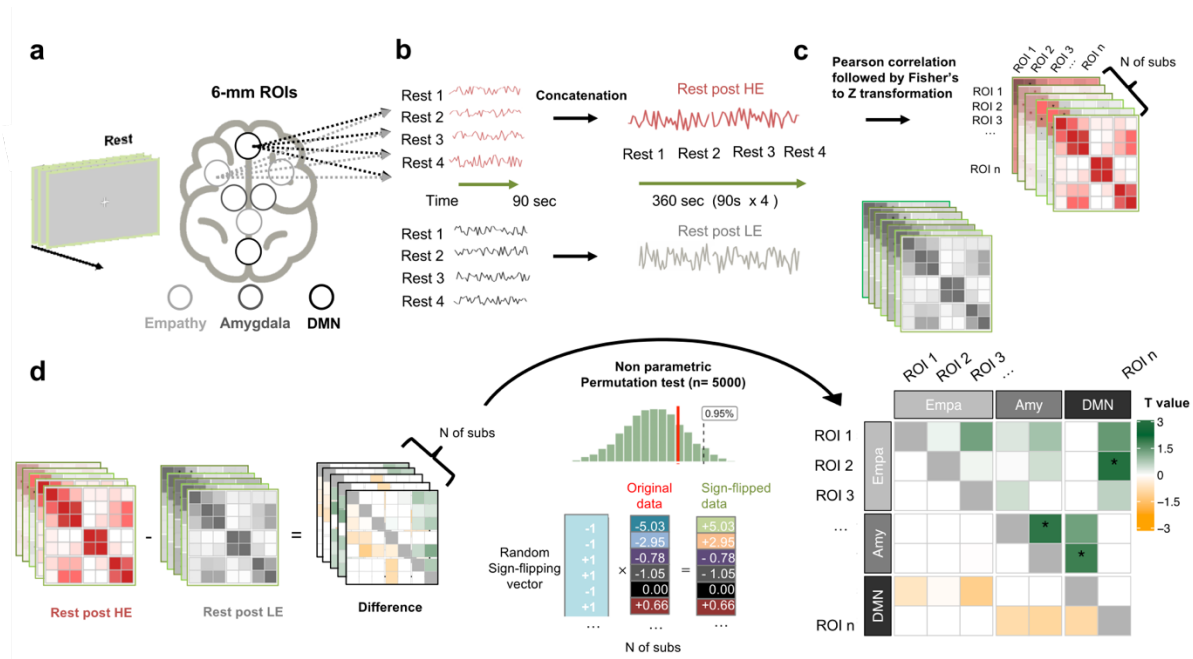
387 For both experiments, we conducted functional connectivity analyses between the most
388 important brain regions of interest (ROIs) associated with the empathy network and with the
389 default mode network (DMN). In addition, we also included the bilateral amygdalae among
390 regions used for this analysis because previous studies assessing carryover effects in the brain
391 have related sustained amygdala activity to anxiety traits ¹⁹ and emotional reactivity ³⁸. For
392 nodes of the DMN, we chose the posterior cingulate cortex (PCC) and the anterior medial
393 prefrontal cortex (aMPFC), following Andrews-Hanna and colleagues ⁷². Based on the results
394 of a meta-analysis by Fan and colleagues ⁵⁰, the bilateral anterior insula (AI) and anterior
395 medial cingulate cortex (aMCC) were used as ROIs in the empathy network. Time series were
396 extracted from 6 mm-radius spheres around the peak of each of these ROIs. The amygdala
397 was defined anatomically using the current SPM anatomical template provided by
398 Neuromorphometrics, Inc (<http://Neuromorphometrics.com/>).

399 Functional connectivity analyses were performed using Matlab 2017 and R studio
400 (version 3.6.1). For each participant, time courses of activity (from each voxel of the brain)
401 were high-pass filtered at 256 Hz, detrended and standardized (*Z*-score) before extracting
402 specific time courses from the defined ROIs. In addition, white matter (WM), cerebrospinal

403 fluid (CSF) signals, and realignment parameters were included as nuisance regressors in
404 Experiment 2. For each participant, time series from the instructions and videos periods were
405 removed, and the remaining time series corresponding to the rest periods were concatenated.
406 This procedure was previously proposed by Fair and colleagues ⁷³ and proved to be
407 qualitatively and quantitatively very similar to continuous resting-state data. Additionally, to
408 correct extreme head motion without affecting the autocorrelation of the time series, image
409 volumes flagged with FD > 0.5mm were removed and replaced by interpolation (every
410 flagged volume X was replaced by the estimated mean of the X-1 and X+1 volumes). The
411 final concatenated time series resulted in 184 frames (~386 s) of resting-state data for each
412 subject.

413 We then correlated the time-courses between the different ROIs using Pearson
414 correlations ⁷⁴, and the resulting coefficients were Fisher's r to z transformed in order to
415 improve normality in the data. Individual Z-score maps (correlation matrices) were created for
416 each participant (see Fig. 2a,b,c). To test for significant differences between the two
417 correlation matrices (post HE rest and post LE rest), we used a non-parametric permutation
418 test ⁷⁵. For each pair of nodes, the permutation test compared the true correlation difference
419 (e.g., HE - LE) to a null distribution built by randomly flipping the sign of the correlation
420 coefficients and computing the difference many times ($n=5000$) (see Fig. 2d). More precisely,
421 for each pair of nodes (e.g., HE - LE for ROI 1 and ROI 3), a vector of values of n =number of
422 participants was obtained and a one-sample t -test was computed to obtain the real t value (t
423 _{real}). Then, the signs of the elements in the vector were randomly flipped ($n=5000$) and the
424 model was fitted repeatedly once for every flipping. For each fit, a new realization of the t
425 statistic was computed so that an empirical distribution of t under the null hypothesis was
426 constructed (t _{permuted}). From this null distribution, a P value was computed by assessing the
427 probability of the t _{real} to be higher than 95% of the values on the empirical t _{permuted}
428 distribution ⁷⁵. Finally, the obtained P values were converted into an equivalent Z-score and
429 significant changes (marked by asterisk in matrices) were retained for $Z > 1.64$ (equivalent to
430 $P < 0.05$, one-tailed given observed increases without decreases in GLM analysis,
431 uncorrected).

432



433

434

435

436

437

438

439

440

441

442

443

444

445

446

447

448

449

Figure 2. Functional connectivity pipeline: (a) Regions of interest (ROIs) from the default mode network (DMN) were chosen based on Andrews-Hanna et al. (2010), including the posterior cingulate cortex (PCC, -8 -56 26) and anterior medial prefrontal cortex (aMPFC, -6 52 -2). ROIs from the empathy network (Empa) were based on the meta-analysis by Fan et al. (2011), including the bilateral anterior insula (AI, -36 16 2 and 38 24 -2) and anterior mid cingulate cortex (aMCC, -2 24 38). A 6 mm-radius sphere was created for each ROI. The amygdalae (Amy) were defined anatomically using the SPM anatomical template. (b) For every participant, time-series from the video and instruction periods were removed, and the remaining time series corresponding to the rest periods were concatenated⁷³. The final concatenated time series of the four rest blocks for each type of video (high emotion, HE or low emotion, LE) resulted in 184 frames (~360 s) of resting-state data for each subject. (c) We then correlated the time-courses between the different ROIs using Pearson's r correlation, and the resulting coefficients were Fisher's r to z transformed to improve normality in the data. Individual Z-score maps (correlation matrices) were created for each participant. (d) Finally, significant differences between the two correlation matrices (Rest post HE vs. Rest post LE) were tested using a non-parametric permutation test⁷⁵. For each pair of nodes, the permutation test compared the true correlation difference t_{real} (HE vs. LE) to a null distribution t_{permuted} constructed by randomly flipping the sign of the correlation coefficients and repeating the t statistic ($n=5000$).

450

451 **Thought probes**

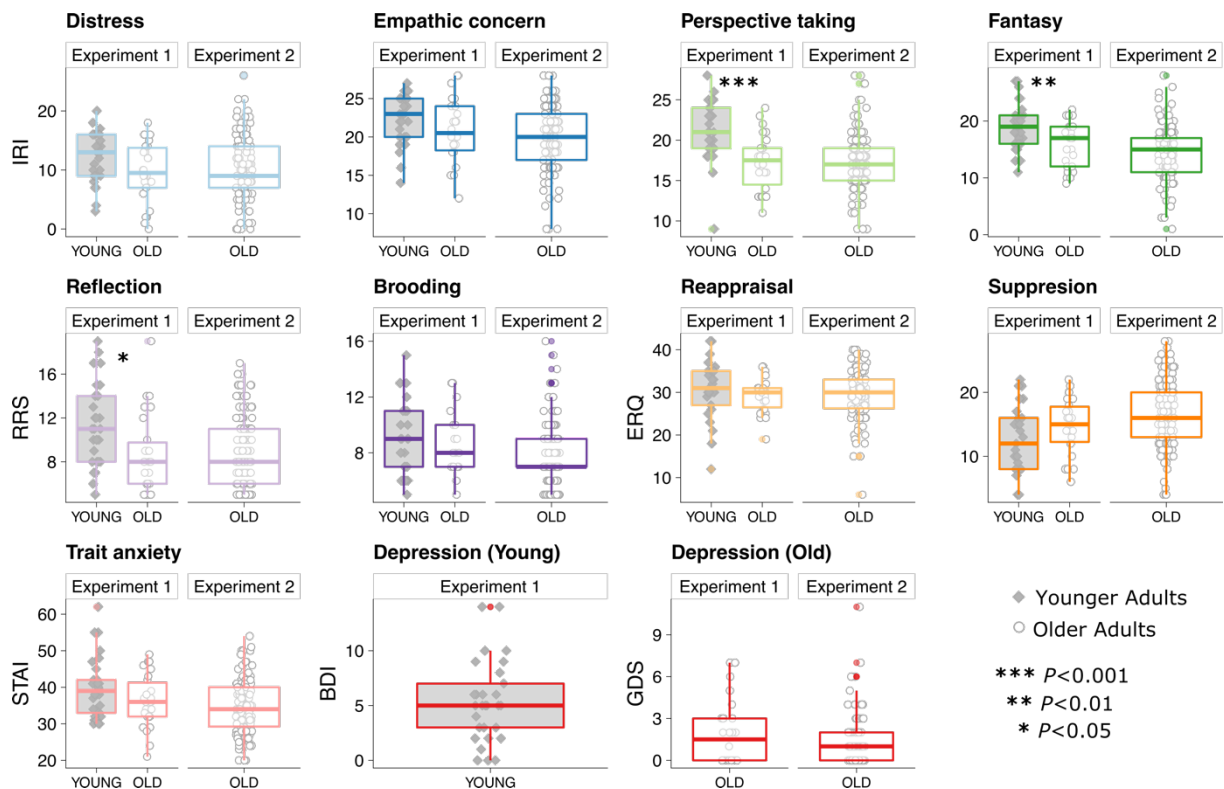
452 For each participant in Experiment 2, two thought probes were recorded after the last rest
453 period of each run and subsequently analyzed to test for differences in spontaneous mind
454 wandering after emotional videos. Participants freely described their thoughts, and these
455 narratives were digitally recorded and transcribed for analyses by two independent raters (see
456 supplementary Table 4). For each probe (post HE rest and post LE rest), the two raters
457 attributed the presence (Present) or the absence (Absent) of specific thought contents
458 according to a diverse set of pre-defined categories (Supplementary Table 4). These
459 categories were selected according to a priori relevant affective or cognitive dimensions, and
460 included the following: *negative and positive emotions, directed attention to oneself and to*
461 *others, emotion regulation (voluntary control of emotions), negative and positive social*
462 *emotions, rumination, and temporality (present or past/future)*. Categories with low
463 variability (i.e., the same thought content reported by more than 85% of participants) were not
464 included in further analyses since this prevented reliable regression analysis (for details, see
465 supplementary Table 4). The final dimensions included *negative and positive emotions,*
466 *directed attention to oneself and to others,* and *positive social emotions*. This final analysis of
467 thought probes comprised data from 109 participants for rest periods after HE videos and 110
468 participants for the rest periods after LE videos. This was due to i) missing thought probes for
469 9 participants and ii) exclusion of reports that did not refer directly to thoughts or feelings in
470 the rest period (but rather to factual details in the videos) for both runs ($n = 5$), following LE
471 rest ($n = 3$) or following HE rest ($n = 4$). Interrater agreement on the final dimensions ranged
472 from 0.28 to 0.66 (Cohen's kappa index; supplementary Table 4 for details). The statistical
473 analyses were performed with R studio (version 3.6.1) and the corresponding graphs were
474 created with ggplot2 (version 3.2.1).

475

476 RESULTS

477 **Participants characteristics**

478
 479 Participants' characteristics, including demographical data, psycho-affective traits, cognitive
 480 abilities, socio-emotional questionnaires, as well as corresponding age differences, are
 481 provided in Table 1 and Fig. 3. Older vs. younger participants (Experiment 1) did not differ in
 482 trait anxiety, affective empathy, and emotion regulation scores. However, older adults
 483 reported lower scores of cognitive empathy as measured by the perspective-taking subscale
 484 ($t_{53} = 4.2, P < 0.001, d = 1.13$, two-tailed) and the fantasy scales of the IRI ($t_{52.3} = 3,$
 485 $P = 0.004, d = 0.81$, two-tailed). Older adults also had lower scores in reflective rumination
 486 ($t_{52.7} = 2.62, P = 0.01, d = 0.7$, two-tailed). The two independent older adults samples
 487 (Experiment 1 and Experiment 2) did not differ in any of the scores (all $t \leq 1.6$, all $P \geq 0.09$).
 488
 489



490
 491
 492 **Figure 3.** Participants' characteristics in terms of psycho-affective traits and socio-emotional competencies for
 493 both Experiment 1 (n=29 younger and n=26 older adults) and Experiment 2 (N=127 older adults). Age-related
 494 differences (Experiment 1) were tested with *t*-tests and significant results are marked with *. Grey diamonds=
 495 younger adults, white dots= older adults. IRI: Interpersonal Reactivity Index, GDS: Geriatric Depression Score
 496 (for older adults only), BDI: Beck's Depression Inventory(for younger adults only), STAI: STAI-trait Anxiety
 497 Index, RRS: Rumination Response Scale, ERQ: Emotion Regulation Questionnaire.

499 Behavioral responses of the SoVT-Rest task

500
501

502 Reliability of the three parallel video sets

503

504 To check whether the three video sets elicited similar emotional responses, we performed
505 repeated measures multivariate analysis of variance (MANOVA, with Pillai's trace statistics)
506 with the within-subject factor “video type” (HE vs LE), the between-subject factor “video set”
507 (V1, V2, V3), and three dependent variables: empathy, positive affect, and negative affect
508 ratings. As expected, and replicating results from Klimecki and colleagues⁵⁵, these analyses
509 revealed no significant differences between the three video sets for any of the self-reported
510 ratings for Experiment 1 (Pillai's trace = 0.07, $F(6,102) = 0.7$, $P = 0.6$) nor for Experiment 2
511 (Pillai's trace = 0.07, $F(6,246) = 1.41$, $P = 0.2$) (see supplementary Fig. 1).

512

513 Impact of high compared to low emotion videos and aging effects on affective and 514 empathy ratings

515

516 In Experiment 1, we compared the effects of HE and LE videos using pairwise *t*-tests for each
517 of the three affective ratings (empathy, positive, and negative affect). These findings were
518 fully replicated in Experiment 2. As predicted, participants reported higher levels of empathy
519 (Exp 1: $t_{54} = 14.35$, $P < 0.001$, $d = 1.67$, two-tailed ; Exp 2: $t_{126} = 14.5$, $P < 0.001$, $d = 1.31$,
520 two-tailed), higher negative affect (Exp 1: $t_{54} = 23.35$, $P < 0.001$, $d = 3.77$, two-tailed; Exp 2:
521 $t_{126} = 26.9$, $P < 0.001$, $d = 2.89$, two-tailed), and lower positive affect (Exp 1: $t_{54} = -16.85$, P
522 < 0.001 , $d = -2.31$, two-tailed; Exp 2: $t_{126} = -18.9$, $P < 0.001$, $d = -2.31$, two-tailed), when
523 presented with HE as compared to LE videos (see Fig. 4a). Importantly, the reported
524 differences between HE > LE conditions on these ratings were not affected by sex in any of
525 the experiments (see supplementary Fig. 6). These data validate a successful elicitation of
526 socio-emotional responses with the SoVT-Rest.

527

528 Additionally, Experiment 1 allowed us to determine age-dependent differences in affective
529 and empathy ratings in the SoVT-Rest task. First, independent ANOVAs showed significant
530 main effects of age on empathy ($F(1,53) = 10.8$, $P = 0.002$) and positive affect ($F(1,53) = 24$,
531 $P < 0.001$), but not on negative affect ($F(1,53) = 1.01$, $P = 0.3$). Follow-up two-sample *t*-tests
532 revealed that in contrast to younger adults, older adults reported higher levels of empathy only
533 for LE videos ($t_{51.5} = 4.45$, $P < 0.001$, $d = 1.19$, two-tailed) as well as higher positive emotions

534 for both HE videos ($t_{36.5} = 4.63$, $P < 0.001$, $d = 1.29$, two-tailed) and LE videos ($t_{50.1} = 3.68$,
535 $P < 0.001$, $d = 0.98$, two-tailed). Interestingly, the two independent older samples
536 (Experiment 1 and Experiment 2) did not differ in any of the scores (all $t \leq 1.8$, all other $P \geq$
537 0.07) (see Fig. 4a) except for even higher ratings of empathy for LE videos in the elderly from
538 Experiment 2 than those from Experiment 1 ($t_{36} = 2.20$, $P = 0.03$, $d = 0.47$, two-tailed).

539

540 We further tested whether age effects on affective ratings were observed within each age
541 group independently (young and older participants). Spearman correlations were computed
542 between age (as a continuous variable) and empathy, positive affect, and negative affect for
543 each age group (collapsing both older adults samples from Experiments 1 and 2). This
544 analysis revealed that during HE videos, age correlated negatively with negative affect ($\rho =$
545 -0.2 , $P_{\text{FDR}} = 0.03$) and positively with positive affect ($\rho = 0.25$, $P_{\text{FDR}} = 0.006$) in older
546 individuals, but not in younger adults. In addition, age correlated positively with empathy for
547 LE videos in the young ($\rho = 0.44$, $P_{\text{FDR}} = 0.03$), but not older adults (Fig. 4b).

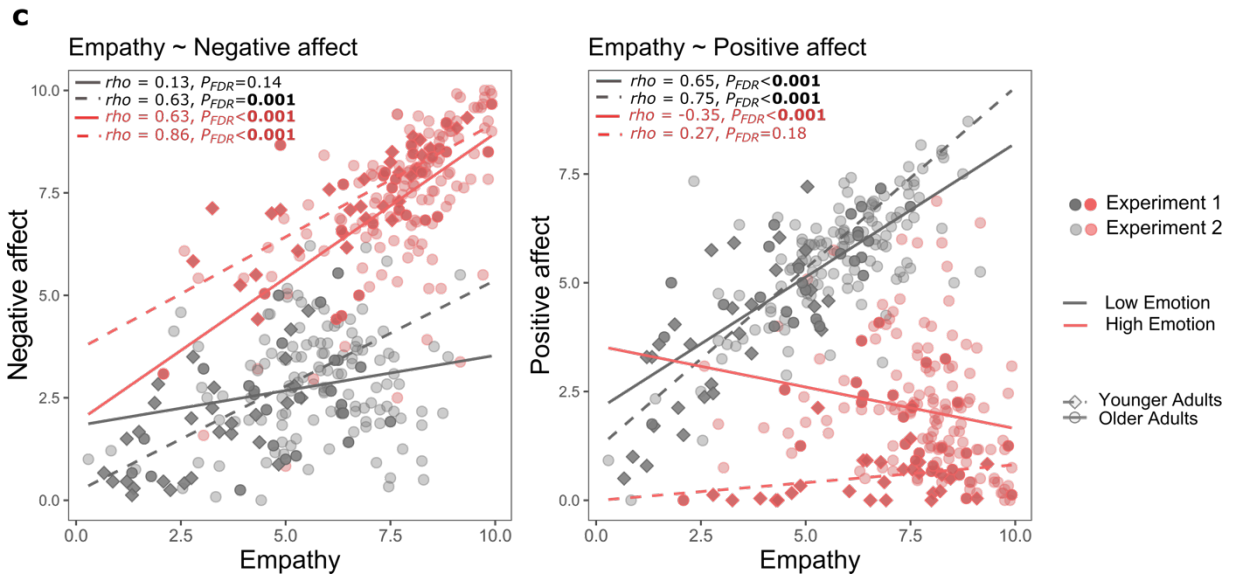
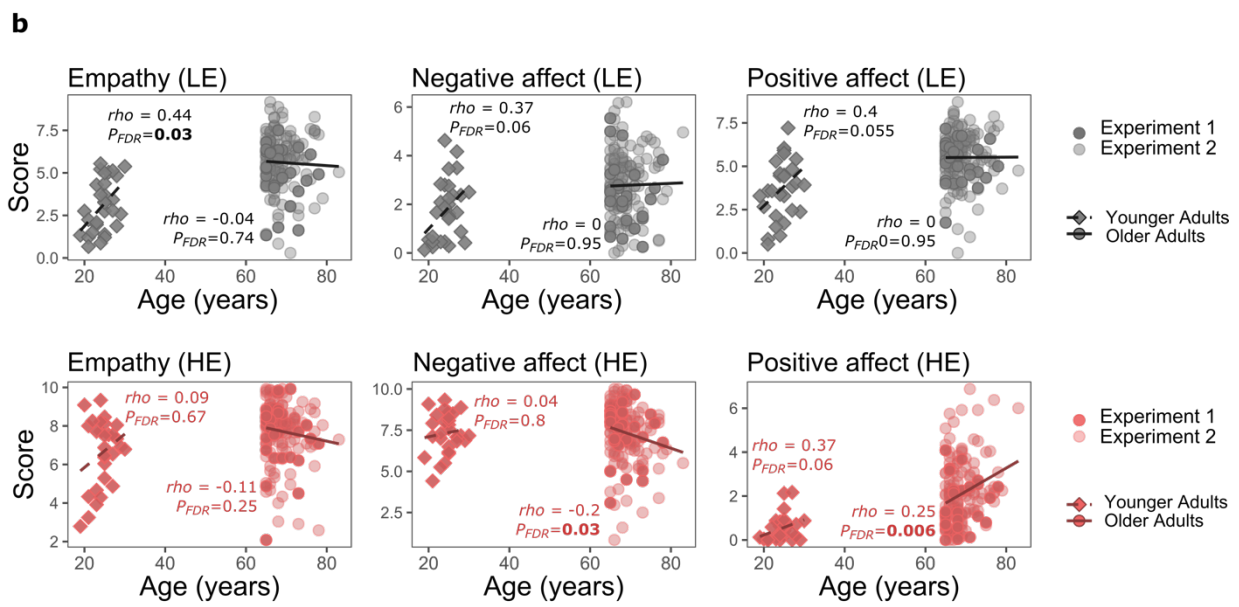
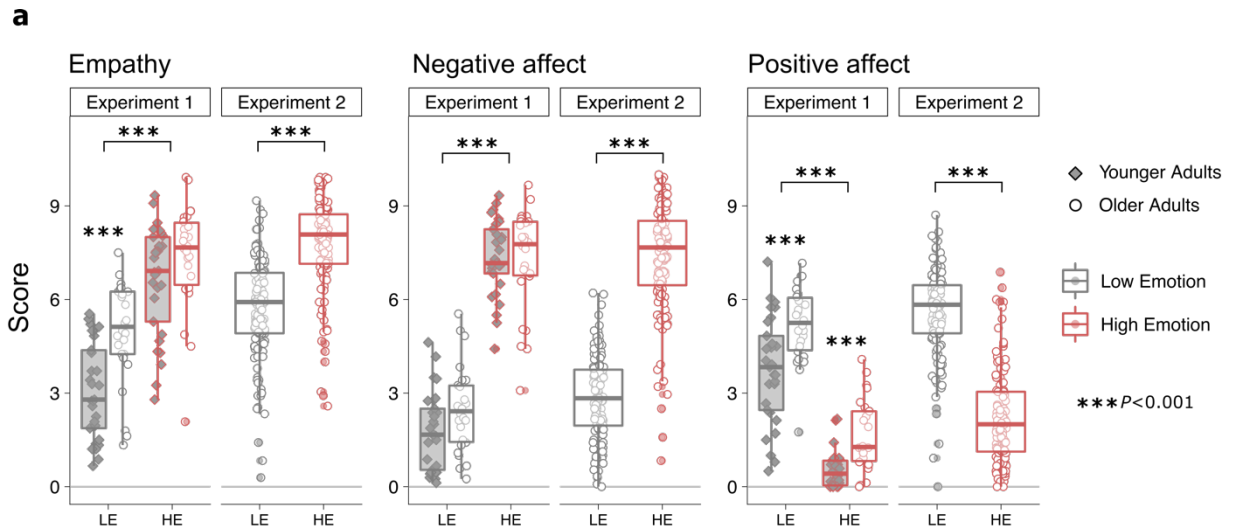
548

549 These analyses were repeated excluding $n=8$ older adults that reported “moderated” levels of
550 depression according to a threshold of GDS > 7 ⁶. Results did not change (see supplementary
551 Table 5). We, therefore, decided not to exclude them from the main analyses.

552

553 **Correlation between empathy and affective valence during the SoVT-Rest**

554 To test how empathy was associated with positive and negative affect during HE and LE
555 videos, we computed Spearman correlations between these rating scales. For both younger
556 and older adults, empathy increased with higher negative affect during HE videos (YOUNG :
557 $\rho = 0.86$, $P_{\text{FDR}} < 0.001$; OLD: $\rho = 0.63$, $P_{\text{FDR}} < 0.001$) and with higher positive affect
558 during LE videos (YOUNG: $\rho = 0.75$, $P_{\text{FDR}} < 0.001$; OLD: $\rho = 0.65$, $P_{\text{FDR}} < 0.001$).
559 Interestingly, during HE videos, empathy correlated negatively with positive affect for older
560 ($\rho = -0.35$, $P_{\text{FDR}} < 0.001$) but not younger adults ($\rho = 0.27$, $P_{\text{FDR}} = 0.18$); whereas during
561 LE videos, empathy correlated positively with negative affect for the younger ($\rho = 0.63$,
562 $P_{\text{FDR}} < 0.001$) but not the older ($\rho = 0.13$, $P_{\text{FDR}} = 0.14$) (Fig. 4c).



564 **Figure 4. (a)** Self-reported scores of empathy, positive affect, and negative affect for the high emotion (HE) and
565 low emotion (LE) videos across experiments. Significant differences between age groups or video type are
566 marked by *** representing $P < 0.001$ (b) Scatter plots illustrating Spearman correlations between age and
567 scores of empathy, positive affect, and negative affect. (c) Scatter plots illustrating Spearman correlations
568 between scores of empathy and affective ratings. Correlations for (b) and (c) were computed together; therefore,
569 P values are reported corrected for multiple comparisons using the false discovery rate (FDR) method.
570 Significant P values are marked in bold. Dots represent averaged values for each participant per condition;
571 Dots/solid line: older adults, diamonds/dashed line: younger adults; $n_{Exp1} = 55$, $n_{Exp2} = 127$; Red: HE videos,
572 Grey: LE videos.
573

574 **Neural responses of the SoVT-Rest task**

575 **Main effects of videos and rest periods (manipulation check)**

576 We first verified that video and rest periods induced differential brain activity by testing for
577 the main effects of task conditions. As expected, comparing videos versus rest periods
578 (Videos > Rest, voxel-wise $P < 0.05$ FWE-corrected) revealed greater activity in widespread
579 networks, including stronger increases in visual cortices. Conversely, comparing rest versus
580 video watching periods (Rest > Videos, voxel-wise $P < 0.05$ FWE-corrected) revealed greater
581 activity in several regions typically associated with the default mode network, such as the
582 PCC/Precuneus, ACC/MPFC, and bilateral IPL. These results were similar in Experiments 1
583 and 2 (see supplementary Fig. 2).

584

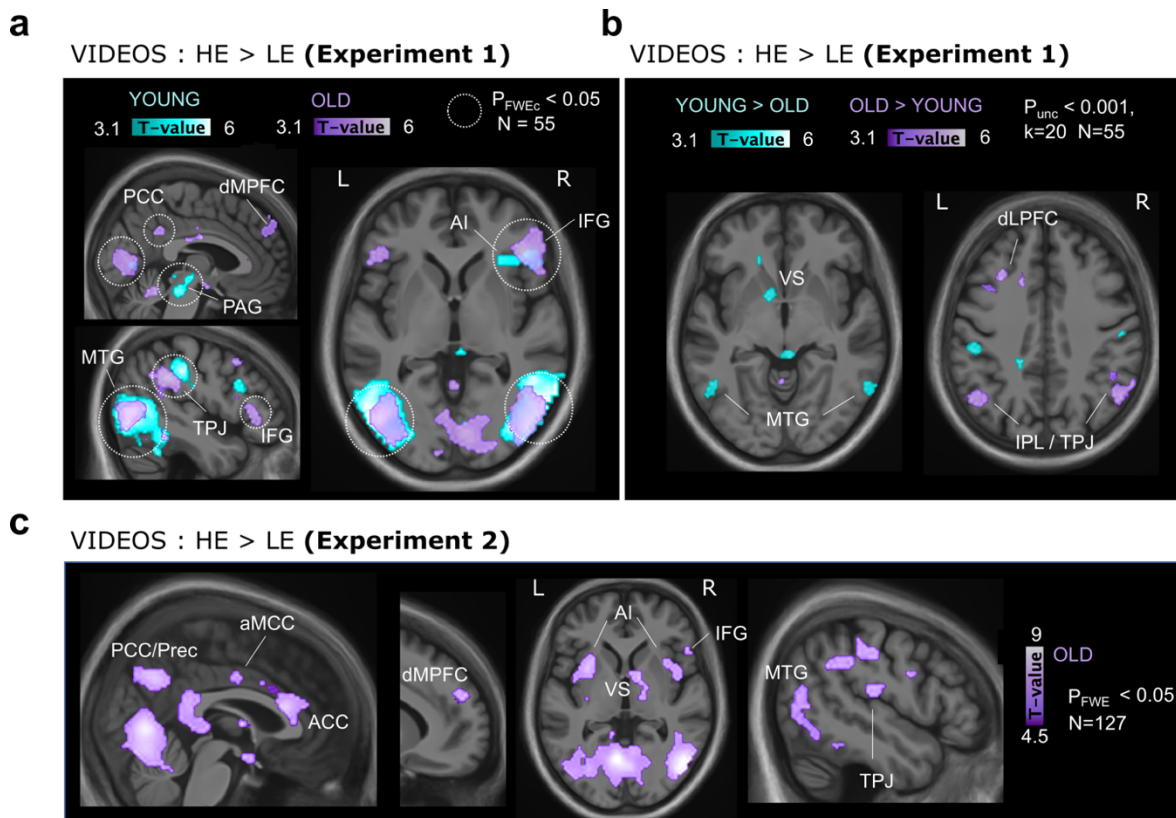
585 **Brain regions activated when faced with others' suffering and age-related** 586 **differences**

587 In Experiment 1, we determined the effect of the emotional content of videos (high, HE vs.
588 low, LE) in each age group, as well as age-related differences. In both groups, the contrast of
589 HE > LE conditions (voxel-wise $P < 0.05$ FWEc-corrected; and $P < 0.001$ uncorrected, $k=20$)
590 demonstrated consistent increases in temporo-parietal junction (l.TPJ), right inferior frontal
591 gyrus (r.IFG), as well as temporal and occipital cortices (see Fig. 5a and supplementary Table
592 3a). Older adults showed larger activations in PCC and dMPFC, whereas younger adults
593 showed additional increases in AI and PAG (see Fig 5a). A direct between-group comparison
594 (2x2 ANOVA) revealed that the older adults more strongly engaged cortical regions in
595 bilateral angular gyrus (TPJ/IPL) and dLPFC. Inversely, the young more strongly engaged
596 subcortical areas in ventral striatum and PAG, as well as sensory areas in parietal and
597 occipito-temporal cortices (Fig 5b).

598
 599
 600
 601
 602
 603
 604
 605
 606
 607
 608
 609

Experiment 2 replicated the results found in older adults from Experiment 1, surviving a more stringent statistical threshold due to the larger sample size. Indeed, HE > LE videos (voxel-wise $P < 0.05$ FWE-corrected) induced greater activity in fronto-parietal and midline regions including left TPJ, dMPFC, and PCC, together with significant increases in bilateral anterior insula (AI), anterior cingulate cortex (ACC), anterior mid-cingulate cortex (aMCC), and ventral striatum (VS) (see Fig. 5c, and supplementary Table 3b).

Overall, brain activations found across the two experiments overlap with networks classically associated with empathy ^{36,50}, compassion ^{55,64,77}, as well as cognitive and affective theory of mind ^{51,78}.



610
 611
 612
 613
 614
 615
 616
 617
 618
 619
 620
 621

Figure 5. Brain regions with greater activation during high emotion (HE) videos in contrast to low emotion (LE) videos across experiments and age groups. **(a)** Brain maps for younger ($n=29$) and older ($n=26$) adults in Experiment 1. **(b)** Between age-groups difference in Experiment 1. For display purposes, results are thresholded at P uncorrected < 0.001 , with a minimum cluster size of ($k = 20$). Clusters surviving correction for multiple comparisons (P FWE < 0.05 at the cluster level) are surrounded in white dotted circles. **(c)** Brain maps for older adults ($N=127$) in Experiment 2. Results survived familywise error (FWE) correction at the voxel level ($P < 0.05$ FWE-corrected). Overall HE > LE videos activated regions previously reported as part of the empathy network (bilateral anterior insula, AI; anterior middle cingulate cortex, aMCC), and regions comprised in the Theory of Mind network (PCC: posterior cingulate cortex, l. TPJ: left temporo-parietal junction, dMPFC: dorsal medial prefrontal cortex) and the Compassion network (VS: ventral striatum) ^{77,79}.

622

623

624 **Older adults show carryover effects of socio-emotional videos during subsequent**
625 **rest periods**

626 To test for carryover effects of emotional videos on subsequent resting state²⁴ and thus assess
627 homeostatic emotion regulation abilities¹⁶, we compared rest periods after HE videos to rest
628 periods after LE videos. In Experiment 1, this contrast (post HE > post LE; voxel-wise $P <$
629 0.001 uncorrected, $k=20$) revealed greater brain activations mostly in the older group,
630 involving the medial prefrontal cortex (MPFC), left anterior insula (l.AI), right inferior frontal
631 gyrus (r.IFG), several temporo parietal cortices, as well as right hippocampus (r.Hipp) (see
632 Fig. 6a and supplementary Table 3a). The same contrast in younger adults showed more
633 limited increases predominating in MCC (see supplementary Table 3a). A direct between-
634 group comparison (2x2 ANOVA) confirmed that older adults engaged these regions (AI, IFG,
635 dMPFC) more strongly, with further significant effects in left MTG and left amygdala,
636 whereas the younger showed higher activity predominating in left hippocampus and precentral
637 motor regions (see Fig 6b and supplementary Table 3a).

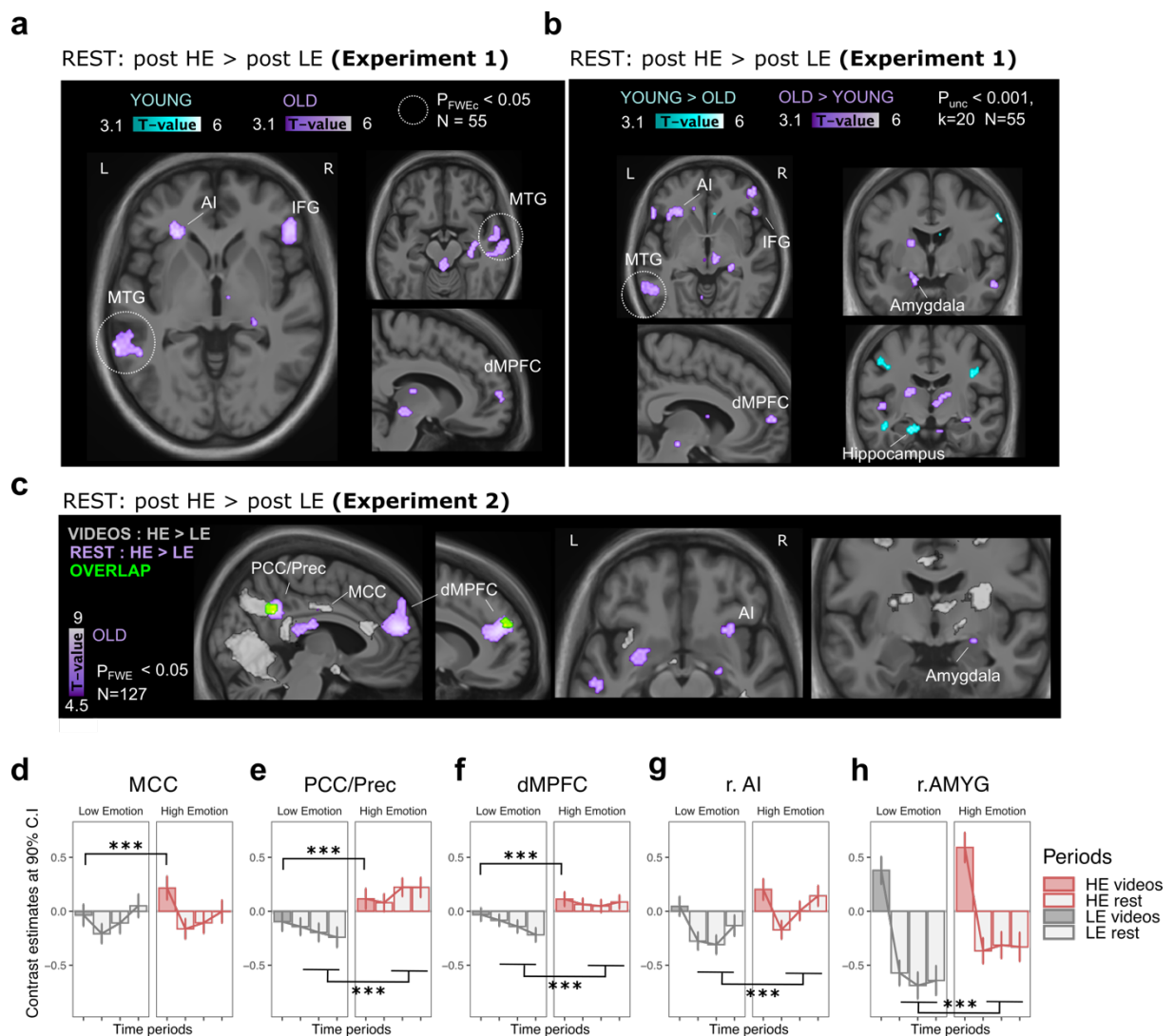
638

639 In Experiment 2, similar regions were found, again surviving a more stringent statistical
640 threshold and replicating our results in older adults from Experiment 1. The contrast post HE
641 > post LE (voxel-wise $P < 0.05$ FWE-corrected) highlighted higher resting activity mainly
642 among midline nodes of the DMN (ACC/dMPFC, and Precuneus/PCC), as well as increases
643 in the right amygdala (r.AMYG) and the ventral part of the right anterior insula (r.AI) (see
644 Fig. 6c and supplementary Table 3b).

645

646 The larger sample size in Experiment 2 allowed us to conduct additional analyses to assess
647 whether these carryover effects at rest directly resulted from higher activity in the same
648 regions during videos periods. To this aim, we identified voxels that were most reliably
649 activated for a specific contrast (HE > LE) across the two periods (videos and rest) by
650 applying an inclusive mask from one contrast (e.g., videos: HE > LE) to the other contrast
651 (rest: post HE > post LE) with a strict threshold used for both ($P < 0.00001$). This overlap of
652 emotional increases (contrasts HE>LE) from both the videos and the rest periods allowed us
653 to determine common areas of activity, shared across the task conditions (Fig. 6c). This
654 analysis revealed a restricted overlap in a few selective regions, mainly dMPFC and PCC,

655 where voxels with emotional activation during videos also exhibited emotional carryover
 656 effects at rest after videos, suggesting sustained increases persisting over time (Fig. 6e,f). In
 657 contrast, other regions differentially activated during emotional videos did not display any
 658 carryover effects during the subsequent rest periods (i.e., exclusively responding to HE > LE
 659 conditions during the videos periods), including not only visual cortical areas but also mid
 660 cingulate areas (MCC; Fig. 6d). Interestingly the right amygdala as well as a segment of the
 661 right anterior insula (ventral part) did not show significant differences for the HE > LE
 662 contrast during videos but were robustly activated in the post HE > post LE rest periods (Fig.
 663 6g,h). These dissociations between rest and video-related activity are further illustrated by
 664 plots of brain activity (contrasts estimates) over time across the different task periods (using a
 665 single time bin of ~45 sec during videos and three successive time bins of 30 seconds during
 666 rest to depict the time course of the activation) and the different conditions (HE and LE
 667 videos) (Fig. 6d,e,f,g,h).
 668



669

670
671 **Figure 6. Carryover effects on brain activity at rest subsequent to high emotion (post HE) versus low**
672 **emotion (post LE) videos across experiments and age groups. (a)** Brain maps for younger adults (n=29, blue
673 clusters) and older adults (n=26, violet clusters) in Experiment 1. **(b)** Direct comparisons of brain maps
674 representing significant age-related differences in Experiment 1. Results are thresholded at P uncorrected $<$
675 0.001, with a minimum cluster size of ($k = 20$). Clusters surviving correction for multiple comparison (P FWE $<$
676 0.05 at the cluster level) are surrounded in white dotted circles. **(c)** Brain activations for older adults (N=127) in
677 Experiment 2. Violet cluster show significant increases in rest periods for the contrast post HE $>$ post LE. Green
678 clusters show the overlap of these activations with emotional effects observed during videos (shown in grey).
679 Results are thresholded at $P < 0.05$ corrected for multiple comparisons using family-wise error (FWE) correction
680 at the voxel level. **(d,e,f,g,h)** Magnitude and time-course of brain activity (parameter estimates) for relevant
681 regions during the different task periods in Experiment 2. **(d)** Example of a region (in MCC) responding to HE
682 vs LE videos, but showing no significant difference during rest after HE vs LE videos. **(e,f)** Example of regions
683 (PCC/Prec and dMPFC) responding to HE $>$ LE videos and showing significant carryover with sustained activity
684 during subsequent rest. **(g,h)** The right amygdala as well as the ventral part of the right anterior insula did not
685 reliably respond to HE vs LE videos but showed significant increases in activations during corresponding rest.
686 Grey lines track activity time-courses during LE conditions. Pink lines track activity time-courses during HE
687 conditions. Grey and pink bars indicate activity (blocks of 3 videos = ~45 seconds) for LE and HE videos
688 respectively, white bars indicate activity (over 3 bins of 30 seconds) during rest periods subsequent to
689 corresponding videos periods. *** $P < 0.05$ FWE-corrected. PCC: posterior cingulate cortex, Prec: precuneus,
690 MCC: mid-cingulate cortex, ACC: anterior cingulate cortex, dMPFC: dorsomedial prefrontal cortex, r. ventral
691 AI: right anterior insula (ventral part), r. AMYG: right amygdala, IFG: inferior-frontal gyrus, MTG : middle
692 temporal gyrus, Hipp: Hippocampus.

693

694 **Exposure to others suffering impacts subsequent brain network connectivity in** 695 **older but not younger adults**

696
697 To further assess the lingering impact of emotional videos on brain activity dynamics
698 (emotional inertia), we examined differences in functional connectivity between and within a
699 priori defined networks. To do so, we first determined the functional connectivity patterns in
700 regional time-series from the default mode network, the empathy network, and bilateral
701 amygdala measured during the rest periods after HE videos, compared to rest periods after LE
702 videos (Fig. 2). We computed connectivity matrices using Pearson correlations between the
703 time-series of every pair of nodes in the three networks of interest. The resulting connectivity
704 matrices obtained for each participant were then group-averaged for illustration (see
705 supplementary Fig. 3). In both experiments, we observed a general pattern of intra-network
706 connectivity (Empa-Empa, Amy-Amy, DMN-DMN) during rest periods subsequent to both
707 the HE and LE videos (see supplementary Fig. 3), consistent with functionally coherent
708 activity within each specific network. To specifically unravel the differential connectivity
709 during rest periods due to emotional inertia (post HE vs post LE rest periods), we directly
710 compared the two connectivity matrices using permutation tests (see methods).

711
712
713
714
715
716
717
718
719
720
721
722
723
724
725
726
727
728
729
730
731
732
733
734
735
736
737
738
739
740
741
742
743
744

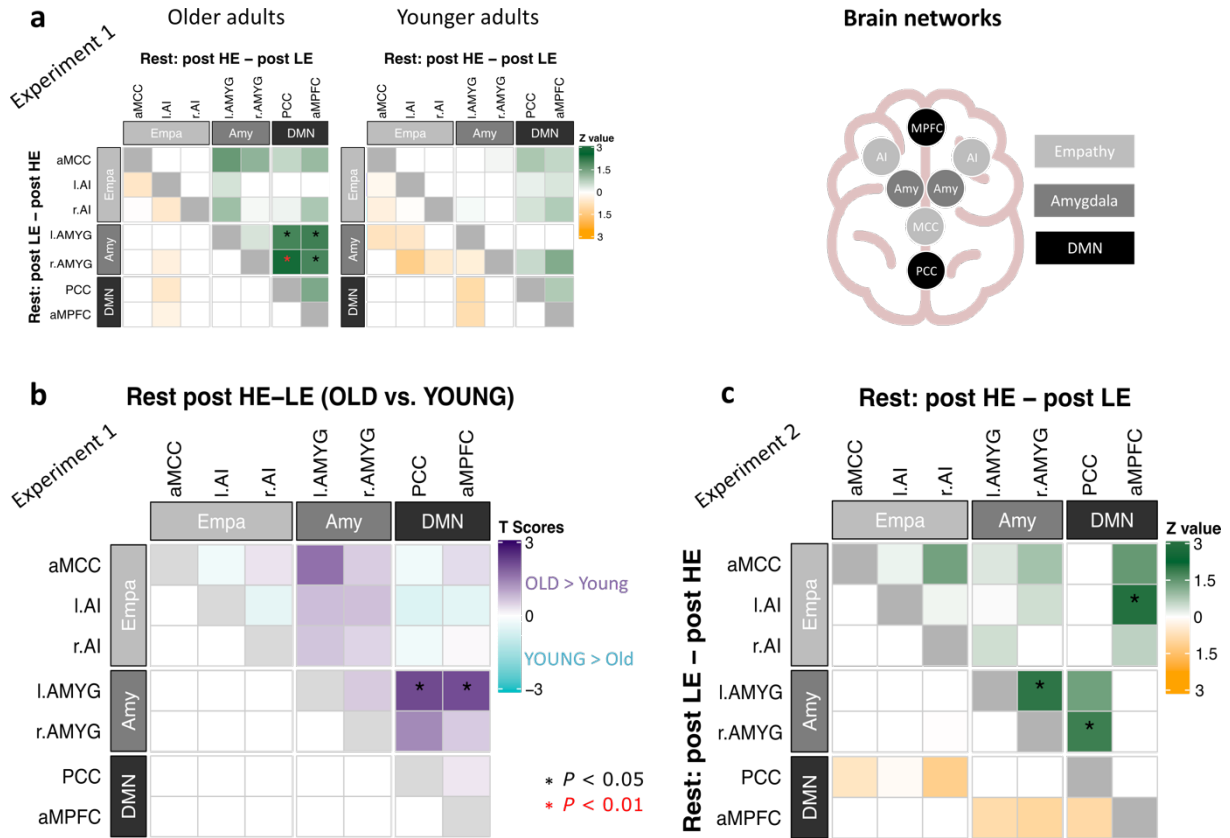
In Experiment 1, significant differences were observed for functional connections of the DMN with bilateral amygdala selectively in older adults: In contrast to post-LE rest periods, resting after HE videos exhibited stronger coupling between the PCC and right amygdala ($t = 2.52, P = 0.008, Z = 2.4$ one-tailed), PCC and left amygdala ($t = 2.1, P = 0.02, Z = 1.97$ one-tailed), as well as between the aMPFC and right amygdala ($t = 2.02, P = 0.03, Z = 1.95$ one-tailed), and between aMPFC and left amygdala ($t = 2.24, P = 0.02, Z = 2.04$ one-tailed) (Fig. 7a). No significant differences in functional connectivity between rest periods after HE and LE videos were found for young adults (see Fig. 7a).

To confirm these age-related differences in functional connectivity patterns, we performed t -tests for each connectivity node between younger and older adults. This direct between-group comparison (Young vs Old: Rest post HE > post LE) showed that, in contrast to younger adults, the older showed significantly larger increases in connectivity between left amygdala and PCC ($t = 2.12, P = 0.03$, two-tailed), as well as left amygdala and aMPFC ($t = 2.08, P = 0.04$, two-tailed) (Fig. 7b).

Experiment 2 revealed similar patterns of increased connectivity in our larger group of elderly. Significant differences were observed for highly selective functional connections of the DMN with limbic areas: In contrast to rest periods after LE videos, rest periods after HE videos induced stronger functional coupling between the PCC and the right amygdala ($t = 1.82, P = 0.03, Z = 1.81$ one-tailed), as well as between the aMPFC and left insula ($t = 1.98, P = 0.02, Z = 2.02$ one-tailed). In addition, there was also higher coupling of the bilateral amygdala during rest periods after HE vs LE videos (right with left, $t = 1.88, P = 0.02, Z = 1.95$ one-tailed) (Fig. 7c).

Because r.AMYG-PCC functional connectivity during rest post HE > LE was significantly increased in older adults from Experiment 1 and this results was replicated in older adults from Experiment 2, we conducted additional t -tests in Experiment 2 that allowed us to assess whether the between-network functional coupling for this pair of nodes was also statistically stronger than for other pairs of nodes including either the right amygdala or the PCC. Results showed that r.AMYG-PCC connectivity was indeed significantly greater than between-network connectivity for other pairs of nodes including left AI-PCC, right AI-PCC and right AMYG-aMPFC (see Fig. 8a).

745



746

747

748

749

750

751

752

753

754

755

756

757

758

759

760

761

762

763

764

765

Figure 7. Functional connectivity (FC) results illustrated as correlation matrices between pairs of ROIs for the different rest conditions in Experiment 1 (a,c) and Experiment 2 (d). **a** Correlation for the difference between the two rest conditions, showing functional coupling between regions for post emotion increases (green) and post emotion decreases (orange) for each age group in Experiment 1, N=55). Left and right halves of the matrix with respect to the diagonal depict the values for inverse contrasts (upper part: post HE - post LE rest periods; lower part: post LE - post HE rest periods). Significant changes in correlations with $Z > 1.64$ are marked by an asterisk * corresponding to $P < 0.05$, one-tailed). **b** Age-related differences between functional connectivity changes (Rest post HE > post LE: Old vs Young) were examined with two sample *t*-tests to identify increases predominating in older adults (OLD > YOUNG, violet) or younger adults (YOUNG > OLD, blue). Significant differences were observed only for older relative to younger adults, depicted by an asterisk * corresponding to $P < 0.05$, two-tailed, uncorrected. **c** Correlation matrix showing significant differences in FC between rest conditions in older adults (N=127) from Experiment 2. The upper right figure illustrates the a priori ROIs selected for the current analysis, including regions from the default mode network, DMN (PCC: posterior cingulate cortex, aMPFC: anterior medial prefrontal cortex.), empathy network, Empa (left and right AI: anterior insula, MCC: anterior mid-cingulate cortex) and bilateral amygdalae, Amy (left and right AMYG).

766 **Relationship between functional connectivity patterns and psycho-affective**
767 **measures**

768

769 Our fMRI connectivity analyses identified a selective impact of emotional videos on
770 functional brain connectivity of the posterior DMN (PCC) with the amygdala, replicated
771 across two independent experiments carried out at different sites. In Experiment 1,
772 connectivity at rest was significantly increased between PCC and bilateral amygdalae in older
773 adults as well as between PCC and left amygdala when directly comparing older to younger
774 adults. In Experiment 2, connectivity was significantly increased between PCC and right
775 amygdala in the larger older sample. These converging results provide a plausible neural
776 mechanism underlying emotional inertia^{16,24} that is specific to older adults and may thus offer
777 a valuable biomarker of homestatic emotion regulation processes in aging.

778

779 In Experiment 2, we could therefore further examine whether this connectivity pattern
780 was related to individual differences in socio-emotional abilities and psycho-affective traits.
781 To do so, we tested for a correlation between the Z-values from significant edges in
782 connectivity matrices (i.e., connections between two ROIs showing a significant difference Z
783 > 1.64 between post HE vs post LE rest) and specific scores on trait anxiety (STAI-trait),
784 rumination (RRS), and empathy (IRI). This analysis showed a significant positive relationship
785 between the magnitude of changes in r.AMYG-PCC connectivity (rest HE – rest LE) and the
786 individual scores of trait anxiety ($r = 0.21$, $P < 0.01$, two-tailed) and rumination ($\rho = 0.22$,
787 $P < 0.01$, two-tailed) (Fig. 8b), but no correlation with empathy ($r = 0.1$, $P = 0.25$, two-
788 tailed).

789

790 **Relationship between functional connectivity patterns and thought probes**

791

792 Because we observed that rumination scores were positively associated with greater changes
793 in functional coupling between r.AMYG-PCC for the contrast post HE $>$ post LE at rest, we
794 reasoned that some participants (i.e., with higher ruminative tendencies) may have kept more
795 negative-related content in their thoughts during the rest periods after emotional videos. This
796 was directly tested in Experiment 2 by using the explicit thought probe given after different
797 rest conditions (see Fig. 1b). To do so, we compared the r.AMYG-PCC connectivity between
798 a subgroup of participants who verbally reported negative content in their spontaneous

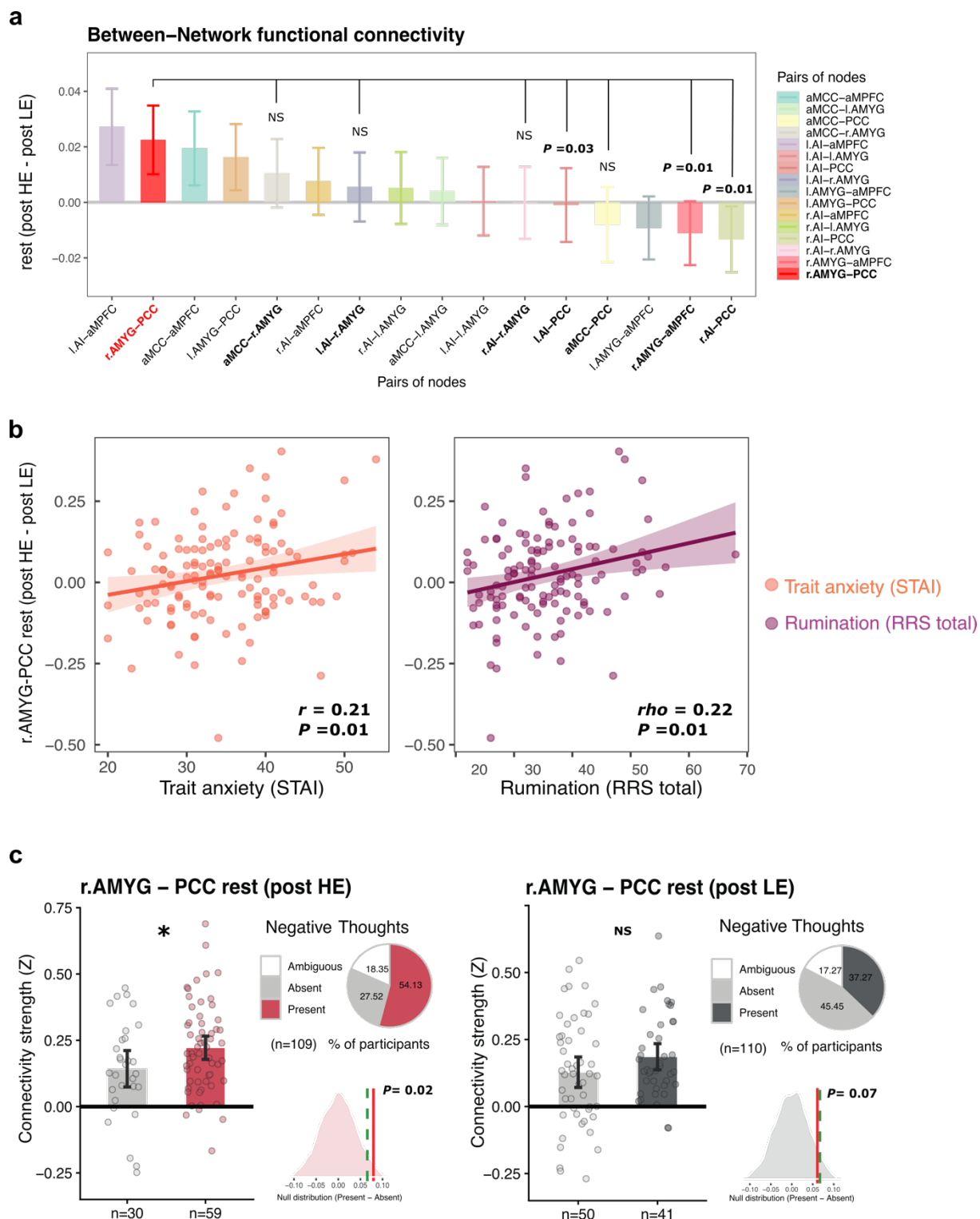
799 thoughts in response to the probe question (Present) vs. those who did not (Absent), for both
800 the HE and LE conditions.

801 Behaviorally, for rest periods after HE videos, 59(54%) participants reported negative
802 thought content, while 30(28%) reported no negative thought content and 20(18%) were
803 ambiguous (judgments by our two raters did not match). Interrater reliability analyses
804 revealed a good agreement ($\kappa=0.61$) between the two independent raters (see
805 supplementary Table 4 for details). A Chi-square test revealed that these proportions
806 (negative present 54% vs. negative absent 28%) were statistically different; $\chi^2(1, N = 109) =$
807 $45.88, P < 0.001$ (two-tailed), demonstrating that HE videos induced more frequent negative
808 than non-negative thoughts in our participants.

809 Conversely, for rest periods after LE videos, only 41(37%) participants reported
810 negative thought content, while 50(45%) reported no negative thoughts, and 19 (17%) were
811 considered ambiguous. The rater agreement was again good ($\kappa = 0.66$) (see
812 supplementary Table 4 for details). This proportion of negative thoughts (37%) was
813 significantly lower than the proportion of non-negative thoughts (45%); Chi-squared test, χ^2
814 $(1, N = 110) = 51.59, P < 0.001$ (two-tailed), indicating that the LE videos induced less
815 frequent negative mental thought content (than non-negative thoughts). An additional
816 McNemar's test further determined that, as expected, participants reported more negative
817 thoughts for rest periods after HE videos than for rest periods after LE videos, $\chi^2 = 10.28, P =$
818 0.02 (two-tailed).

819 Finally, to relate these behavioral indices to brain effects, we used a non-parametric
820 permutation analysis in which the r.AMYG-PCC connectivity difference (*observed diff* =
821 0.08) between these two subgroups (negative thoughts Present-Absent) was compared to a
822 null-distribution built by permuting the labels 5000 times. As hypothesized, we found that the
823 54% of participants reporting negative content in their thoughts (vs. 28% not reporting)
824 showed increased r.AMYG-PCC connectivity for the rest periods following HE videos ($P =$
825 0.02 , one-tailed). The same difference between the two subgroups for rest periods following
826 LE videos was only a trend (*observed diff* = 0.06; $P = 0.07$, one-tailed) (Fig. 8c). Taken
827 together, these findings further unveil a direct relation between r.AMYG-PCC connectivity
828 changes after negative emotions and individual reactivity to aversive or stressful socio-
829 emotional stimuli.

830



831

832 **Figure 8. (a)** Between-network functional connectivity during rest periods after HE > LE videos. Pairs of nodes
 833 are ordered from left to right according to the connectivity strength. In red, the r.AMYG-PCC pair was
 834 significantly more connected than other pairs (but not all) involving either the PCC or the right amygdala (in
 835 bold); significant comparisons from *t*-tests (one-tailed) are marked with corresponding *P* values, NS: not
 836 significant **(b)** Pearson (*r*) and Spearman (*rho*) correlations show that higher functional connectivity between
 837 amygdala and posterior cingulate cortex during rest periods after HE > LE videos [r.AMYG-PCC(rest HE-rest
 838 LE)] was positively related to trait anxiety (STAI) and rumination (RRS total). **(c)** r.AMYG-PCC connectivity
 839 between the group of participants who verbally reported negative content during the thought probes (Present) vs.
 840 the group who did not (Absent), for both HE and LE conditions. After HE videos, 59(54%) participants reported

841 negative content in their thought probes, 30(28%) did not report negative content and 20(18%) were ambiguous.
842 After LE videos, only 41(37%) reported negative content, 50(45)% reported negative thoughts, and 19(17%)
843 were ambiguous. At the brain level, we performed a non-parametric permutation analysis to compare the
844 observed mean r.AMYG-PCC connectivity difference between the two groups Present-Absent (*observed diff* =
845 0.08), relative to a null-distribution built by permuting the labels 5000 times. As hypothesized, we found that
846 54% of the participants reporting negative content in their thoughts (vs. 28% not reporting negative thoughts)
847 showed increased r.AMYG-PCC connectivity in the HE condition ($P = 0.02$, one-tailed). In the LE condition,
848 there was no significant difference in r.AMYG-PCC connectivity between the two groups (*observed diff* = 0.06;
849 $P = 0.07$, one-tailed). Red: High Emotion (HE) condition, Grey: Low emotion (LE) condition. r.AMYG-PCC:
850 connectivity between the right amygdala and the posterior cingulate cortex. Percentages in the text are rounded.
851 Data from Experiment 2.

852

853

854 DISCUSSION

855

856

857 The current study sought to delineate neural markers of emotional resilience and empathy in
858 aging, which are increasingly recognized as important protective factors against mental illness
859 and cognitive decline in this population⁸⁰. We assessed both reactivity and recovery of brain
860 networks to negative socio-affective situations (i.e., during and after videos) in two
861 independent experiments, including a large number of younger and older adults (N=182). In
862 Experiment 1, we focused on validating the task and assessing aging effects on affective
863 processes that allowed us to probe for emotional carryover effects in resting state (emotional
864 inertia) as an indirect indicator of maladaptive regulation processes¹⁶. In Experiment 2, we
865 replicated the results and further examined the relationship between brain carryover effects
866 and measures of anxiety, rumination, and negative thoughts in older adults.

867

868

869 **Aging effects on behavioral characteristics**

870 Overall, our two samples of older adults (Experiment 1 and Experiment 2) did not differ in
871 any of the questionnaires assessing affective or cognitive traits. Compared to younger adults,
872 older adults reported lower scores in cognitive-related processes, including reflective
873 rumination and cognitive empathy. These findings converge with previous work showing a
874 decline of cognitive abilities as people get older, including cognitive components of social
875 functions⁴, while socio-affective abilities tend to remain stable.

876

877 Accordingly, measures of affect and empathy showed largely preserved patterns in the
878 elderly that extend previous findings in younger adults⁵⁵. Seeing videos of others' suffering

879 induced higher levels of negative affect, lower positive affect, and higher empathy scores than
880 mundane scenes of daily life, in both younger and older participants. Nonetheless, age
881 differences were observed, with older adults reporting more positive emotions for both LE
882 and HE videos. Moreover, despite a restricted age range in our elderly population, we found
883 that the older the age, the lower the negative and the higher the positive emotions reported to
884 videos of suffering (see Fig. 4b). This relationship between age and affect was not present for
885 young participants. These results confirm the "positivity bias" often described in the elderly⁷,
886 which may reflect a motivation to upregulate positive and downregulate negative information
887 from emotional stimuli⁷. In contrast, young and older adults reported similar levels of
888 negative affect in response to others' suffering. This suggests that the positivity bias of older
889 adults does not necessarily impair their capacity to feel negative emotions when facing
890 someone who is suffering. This underlines the importance of separately assessing negative
891 and positive emotions, as done in the SoVT-Rest task, an issue already highlighted in
892 previous research^{81,82}

893

894 Finally, we found that emotional responses were modulated by levels of experienced
895 empathy. Higher empathy correlated not only with increased negative affect during HE videos
896 but also with increased positive affect during LE videos, for both older and younger adults
897 (see Fig. 4c). However, positive emotions were reduced with higher empathy during HE
898 videos only in older adults. These results indicate that modulation of positive emotions by
899 empathy in older adults may depend on the context: the higher the empathy, the higher the
900 positive emotions when facing social stimuli without overt emotional content, but the lower
901 the positive emotions when facing social stimuli of others' distress. These data offer a new
902 perspective on how empathy for others' suffering may impact the "positivity bias" usually
903 observed in the elderly.

904

905 **Brain activity markers of empathy and age differences**

906 Exposure to others' suffering (contrast HE > LE videos) engaged several regions overlapping
907 with networks previously associated with social cognition and emotion. These encompassed
908 regions related to affective empathy, pain processing, or more generally salience detection
909 (aMCC, AI), as well as parts of the theory of mind (ToM) network (PCC, r.TPJ, dMPFC,
910 IFG) and the compassion network (ventral striatum)^{77,79}. These results converge with
911 abundant evidence implicating aMCC and AI in empathy for pain^{36,50}, encoding behaviorally

912 salient information ^{83,84} and negative affect ^{85,86}. Likewise, TPJ and dMPFC are consistently
913 engaged in scenarios requiring cognitive abilities to infer others' affective and mental state
914 ^{87,88}, and therefore implicated in cognitive aspects of empathy and theory of mind ^{36,51}. In
915 addition, in younger adults in Experiment 1 and the larger sample of older adults in
916 Experiment 2, the HE>LE videos also activated clusters in ventral striatum, an area associated
917 with positive affect and reward ⁸⁹ and engaged during compassion for other's suffering ^{64,77}.

918

919 Remarkably, despite its prominent role in emotional processing, there was no
920 significant activation in the amygdala during the HE > LE videos in either group. This null
921 result might however accord with the notion that the amygdala responds more broadly to
922 social or self-relevant information rather than just negative valence ^{90,91}, and may already
923 activate to the content of LE videos. This would accord with similar increases seen during
924 both video conditions in Experiment 2 (see supplementary Fig. 2 and Fig. 6h).

925

926 Importantly, age differences were observed in these neural responses. Older adults
927 activated less regions typically related to empathy (AI, PAG) and more those related to social
928 cognition and emotion regulation (DMPFC, PCC, IFG). This adds to a few previous studies
929 that examined age-effects on empathy for pain ^{43,46} and empathy for negative and positive
930 emotions ⁹². Lower activity in affect-related regions, along with higher activity in cognition-
931 related frontal regions have been interpreted as a mechanism for enhanced emotion regulation
932 performance, possibly mediating the positivity bias of older people ^{3,93}. On the other hand,
933 increased activity in frontal regions may also reflect compensatory brain mechanisms acting
934 to overcome cognitive deterioration in older adults (Cabeza, 2002; Davis, 2008). Further
935 research is therefore needed to explicitly test cognitive functioning and clarify how it
936 accounts for this activation pattern in older adults, an issue beyond the purpose of the present
937 study.

938

939 In any case, our findings suggest that socio-affective functions and brain regions
940 mediating empathy and theory of mind exhibit globally normal patterns of engagement in
941 response to negative social situations in the healthy elderly. These data also demonstrate that
942 our video paradigm effectively engaged emotion and empathy processes in our participants,
943 and confirm a positive affective bias of older individuals in both their behavioral and neural
944 responses to social scenes, indicating globally preserved empathy and emotional balance.

945

946 **Emotional inertia and recovery from emotions after exposure to others' suffering**

947
948 Beyond transient responses to negative stimuli, assessing the impact of emotions over time is
949 crucial to determine how people cope with stressful events ⁹⁴. Emotional inertia denotes a
950 persistence of emotional states ¹⁶ reflecting inefficient recovery and greater risk for
951 psychological maladjustment ^{22,94-96}. Although well-studied behaviorally ^{16,20}, emotional
952 inertia remains largely unexplored at the brain level, especially in old populations. To uncover
953 its neural underpinnings, we probed for carryover effects in brain activity at rest following
954 exposure to emotional videos and assessed age-related differences.

955
956 Across our two experiments, we observed selective increases during rest periods after
957 HE relative to LE videos in midline brain areas (ACC/MPFC and Precuneus/PCC), involving
958 core parts of the DMN typically active at rest ⁷², together with increases in amygdala and
959 insula, two regions implicated in emotional processing ³⁷. Importantly, these effects occurred
960 only in older adults, suggesting an important modulation of emotion regulation mechanisms
961 during aging. The DMN is implicated in self-related internally-oriented processes, including
962 memory, interoception, and value-based decision making ^{33,34}. Interestingly, previous research
963 found that the duration of activation in midline DMN regions was a better predictor of the
964 subjective emotional intensity of negative stimuli than the magnitude of activation ²⁶. Other
965 fMRI studies reported modulations of DMN in response to emotional challenges, although
966 with divergent findings. While some researchers reported attenuated DMN activation
967 following various emotions ^{24,25}, others reported increases ^{26,32}, similar to the current results.
968 In Experiment 2, we further found that two midline nodes of DMN (i.e., Precuneus/PCC and
969 dMPFC) were not only activated in the HE > LE contrast during videos, but also continued
970 their activity in the corresponding contrast during subsequent rest (post HE > post LE),
971 providing direct evidence for “emotional inertia” in the aging brain. These findings resonate
972 with previous work showing that older, but not younger, adults fail to deactivate regions of
973 the DMN during cognitive control and visuospatial tasks ^{41,42}. To our knowledge, these data
974 reveal for the first time that increased DMN activations in the elderly can persist over time
975 after exposure to negative socio-emotional contexts.

976
977 Sustained changes were also observed in limbic regions in Experiment 2. The anterior
978 insula showed increased activity during both the (HE > LE) videos and the (post HE > post
979 LE) rest periods, although the voxelwise activations did not fully overlap between the two
980 conditions: while there was a more dorsal engagement during videos, more ventral parts of

981 the anterior insula were active after the emotional event. In light of previous research in
982 younger adults ⁹⁷ suggesting that dorsal AI may be recruited during adaptive behavior
983 mechanisms while ventral AI may be highly recruited during internal homeostatic regulation,
984 our result may reflect a shift from controlled/explicit adaptation to more spontaneous/implicit
985 homeostatic regulation. On the other hand, the amygdala did not differentially respond during
986 the (HE > LE) videos, but it showed a lower return to baseline levels during rest after HE vs.
987 LE videos. Accordingly, prolonged amygdala activity after negative images was reported to
988 predict greater trait neuroticism ³⁸, and enhanced amygdala response to threat faces after
989 negative emotion elicitation is amplified in high anxiety individuals ¹⁹.

990 Altogether, our data highlight the importance of the temporal dynamics of brain
991 responses to emotion in order to determine individual affective styles and risks for
992 psychopathology ^{24,26,29}.

993

994 **Brain connectivity patterns related to emotional inertia**

995

996 Our functional connectivity analysis revealed that post-emotional carryover effects were
997 organized in different circuits, linking core parts of the DMN (PCC and MPFC) with limbic
998 regions (amygdala and anterior insula). These connections were selectively enhanced in post
999 HE relative to post LE rest, exclusively in older adults, and across both experiments (see Fig.
1000 7). These results unveil sustained coupling patterns between the midline DMN and limbic
1001 networks induced by emotional inertia, which were accompanied by distinctive behavioral
1002 features.

1003

1004 The PCC and amygdala were more active and functionally more connected in the post-
1005 emotional rest periods in older adults. Detailed analyses of Experiment 2 revealed that PCC-
1006 amygdala connectivity was stronger for HE than LE conditions, but also selectively stronger
1007 than other between-network connectivity patterns involving either the PCC or the amygdala
1008 (see Fig. 8a). Interestingly, the strength of PCC-amygdala enhanced connectivity was
1009 predicted by individual anxiety and rumination. Older adults reporting higher rumination
1010 tendencies and anxious traits on questionnaires also exhibited stronger PCC-amygdala
1011 connectivity after emotional videos. In addition, explicit verbal reports revealed that more
1012 participants expressed negative thought contents during the rest period that followed HE
1013 videos. Importantly, these participants with more frequent negative thoughts also had higher
1014 PCC-amygdala connectivity than those who reported no negative thoughts, and this was not
1015 the case during rest periods after LE videos. These findings suggest that increased functional
1016 connectivity between PCC and amygdala may directly underpin the persistence of negative
1017 content in spontaneous thoughts.

1018

1019 Past neuroimaging research suggests that PCC is involved in internally directed
1020 cognition, rumination and memory ^{34,98} especially when people retrieve contextual and
1021 affective autobiographical information ^{99,100}. As the amygdala also plays a central role in
1022 affective memory by encoding and storing information about emotional relevance ^{35,90,101}, we
1023 speculate that PCC-amygdala communication may contribute to emotional inertia and
1024 recovery from socio-emotional stressful situations, possibly by associating the content of
1025 vicarious negative experiences to personal affective memories in older adults, and especially
1026 in individuals with higher levels of anxiety and rumination. These data unveil new age-related
1027 effects on neural processes associated with rumination and repetitive negative thinking, i.e.,

1028 mental states implying persistent self-relevant thoughts about negative information ¹⁰² that are
1029 associated not only with maladaptive emotion regulation but also with increased risk of
1030 cognitive decline and Alzheimer's disease ^{12,14}. As neurodegenerative anomalies in PCC and
1031 medial brain regions are commonly seen in Alzheimer's disease ^{103,104}, changes in PCC
1032 connectivity might constitute a possible neural marker for deficient affective resilience, which
1033 is in turn associated with a higher risk for dementia.

1034

1035 Our results thus complement prior work on DMN connectivity in aging populations.
1036 Indeed, recent research demonstrated that functional connectivity between the DMN and
1037 cognitive control regions (dlPFC) was modulated by the cognitive load/efforts on the task in
1038 older but not younger adults ⁴². Our data extend this to affective contexts and link it to
1039 specific psychological traits. Indeed, DMN connectivity to limbic regions is amplified after
1040 emotional induction in older (but not younger) adults, with PCC-amygdala coupling being
1041 distinctively sensitive to anxiety, rumination, and self-reports of negative thoughts.

1042

1043 In parallel, increased functional connectivity was also observed between AI and
1044 aMPFC after HE compared to LE videos in the larger older adult sample from Experiment 2.
1045 These neural changes showed no correlation with anxiety or rumination but only a weak
1046 positive correlation with the empathic concern IRI subscale (see supplementary Fig. 4). These
1047 findings may reflect a more general role of AI in emotional awareness ^{105,106} and empathy ³⁶,
1048 and of aMPFC in the representation of affective states in both the self and others ^{78,107}. These
1049 results extend prior work by showing that modulation of connectivity between these two
1050 regions may occur not only during the appraisal of socio-emotional stimuli but also persist
1051 beyond emotional events.

1052

1053 LIMITATIONS AND FUTURE DIRECTIONS

1054 Some limitations of our study need to be acknowledged. First, we explicitly instructed
1055 participants to watch videos passively, and therefore some of the subsequent carryover effects
1056 on brain activity and connectivity could be interpreted as unsuccessful implicit emotion
1057 regulation styles inherent to the participants. It would be interesting to assess in future studies
1058 whether instructing participants with explicit emotion regulation strategies may change the
1059 subsequent brain response related to emotional inertia. Second, technical constraints of the
1060 fMRI scanner also engendered some limitations. First, as explained in the methods, we

1061 obtained affective ratings on videos outside of the scanner, immediately after the scanning
1062 session. Although this may bias how participants rated the videos, we deliberately made the
1063 choice in order to 1) avoid top-down cognitive influences during scanning which may
1064 confound neural activity during emotional perception ^{65,66}; and 2) maximize older adults'
1065 comfort by reducing the time spent inside the scanner (particularly because other anatomical
1066 and functional MRI sequences including T1, T2 and T2* were carried out during the same
1067 session). Second, as described in supplementary Fig. 5, some basal forebrain voxels were
1068 automatically excluded from our group analyses in Experiment 2, due to magnetic field
1069 inhomogeneities frequently induced in brain regions near air-filled cavities in the human head
1070 ¹⁰⁸. Consequently, we were not able to reliably study regions such as the orbitofrontal cortex
1071 (OFC), which plays an essential role in positive emotions and reward ^{64,89}.

1072

1073 CONCLUSION

1074

1075 In sum, our study demonstrates that empathy for suffering and affective resilience can reliably
1076 be investigated in the elderly using the SoVT-Rest, a novel paradigm that has very low
1077 cognitive load and high ecological validity for applications in frail or clinical populations.
1078 Using the SoVT-Rest, we find neural and behavioral markers of the positivity bias in the
1079 elderly and show for the first time sustained carryover effects (or emotional inertia) in
1080 corticolimbic brain circuits in populations of healthy older adults. Interestingly, PCC and
1081 amygdala's functional connectivity at rest was increased during high emotional events, and
1082 such increase was related to anxiety, rumination, and negative thought content, making this
1083 resting connectivity pattern a highly likely neural substrate for emotional inertia. These
1084 findings provide an important cornerstone for better understanding empathy and mechanisms
1085 underlying affective resilience in the brain of the elderly population, and thus contribute to
1086 identifying potential risk markers for neurodegenerative diseases associated with poor social
1087 stress coping.

1088 DATA AVAILABILITY

1089

1090 The data underlying this report are made available on request following a formal data sharing
1091 agreement and approval by the consortium and executive committee
1092 (<https://silversantestudy.eu/2020/09/25/data-sharing>). The Material can be mobilized, under
1093 the conditions and modalities defined in the Medit-Ageing Charter, by any research team

1094 belonging to an Academic for carrying out a scientific research project relating to the
1095 scientific theme of mental health and well-being in older people. The Material may also be
1096 mobilized by non-academic third parties, under conditions, in particular financial, which will
1097 be established by separate agreement between Inserm and by the said third party. Data sharing
1098 policies described in the Medit-Ageing Charter are in compliance with our ethics approval
1099 and guidelines from our funding body.

1100

1101 CODE AVAILABILITY

1102

1103 The code used to produce the results reported in the manuscript can be made available upon
1104 appropriate request.

1105

1106 REFERENCES

1107

- 1108 1. Glisky, E. Changes in Cognitive Function in Human Aging. 3–20 (2007).
1109 doi:10.1201/9781420005523.sec1
- 1110 2. Carstensen, L. L., Mayr, U., Pasupathi, M. & Nesselroade, J. R. Emotional experience
1111 in everyday life across the adult life span. *J. Pers. Soc. Psychol.* **79**, 644–655 (2000).
- 1112 3. Mather, M. The Affective Neuroscience of Aging. (2015). doi:10.1146/annurev-psych-
1113 122414-033540
- 1114 4. Reiter, A. M. F., Kanske, P., Eppinger, B. & Li, S.-C. The Aging of the Social Mind -
1115 Differential Effects on Components of Social Understanding. *Sci. Rep.* **7**, 11046
1116 (2017).
- 1117 5. Urry, H. L. & Gross, J. J. Emotion regulation in older age. *Curr. Dir. Psychol. Sci.* **19**,
1118 352–357 (2010).
- 1119 6. Lang, F. R. & Carstensen, L. L. Time counts: Future time perspective, goals, and social
1120 relationships. *Psychol. Aging* **17**, 125–139 (2002).
- 1121 7. Mather, M. & Carstensen, L. L. Aging and motivated cognition: The positivity effect in
1122 attention and memory. *Trends in Cognitive Sciences* **9**, 496–502 (2005).
- 1123 8. Aldao, A., Nolen-Hoeksema, S. & Schweizer, S. Emotion-regulation strategies across
1124 psychopathology: A meta-analytic review. *Clin. Psychol. Rev.* **30**, 217–237 (2010).
- 1125 9. Hamilton, J. P., Farmer, M., Fogelman, P. & Gotlib, I. H. Depressive Rumination, the
1126 Default-Mode Network, and the Dark Matter of Clinical Neuroscience. *Biol.*
1127 *Psychiatry* **78**, 224–230 (2015).
- 1128 10. Kraaij, V., Pruyboom, E. & Garnefski, N. Cognitive coping and depressive
1129 symptoms in the elderly: A longitudinal study. *Aging Ment. Heal.* **6**, 275–281 (2002).
- 1130 11. Terracciano, A. *et al.* Personality and risk of Alzheimer’s disease: New data and meta-
1131 analysis. *Alzheimer’s Dement.* **10**, 179–186 (2014).
- 1132 12. Marchant, N. L. & Howard, R. J. Cognitive debt and Alzheimer’s disease. *J.*
1133 *Alzheimer’s Dis.* **44**, 755–770 (2015).
- 1134 13. Wilson, R. S., Begeny, C. T., Boyle, P. A., Schneider, J. A. & Bennett, D. A.
1135 Vulnerability to Stress, Anxiety, and Development of Dementia in Old Age. *Am. J.*
1136 *Geriatr. Psychiatry* **19**, 327–334 (2011).

- 1137 14. Marchant, N. L. *et al.* Repetitive negative thinking is associated with amyloid, tau, and
1138 cognitive decline. *Alzheimer's Dement.* 1–11 (2020). doi:10.1002/alz.12116
- 1139 15. Jané-Llopis, E. *et al.* *Mental Health in Older People.* (2008).
- 1140 16. Kuppens, P., Allen, N. B. & Sheeber, L. B. Emotional inertia and psychological
1141 maladjustment. *Psychol. Sci.* **21**, 984–991 (2010).
- 1142 17. Koval, P., Kuppens, P., Allen, N. B. & Sheeber, L. Getting stuck in depression: The
1143 roles of rumination and emotional inertia. *Cogn. Emot.* **26**, 1412–1427 (2012).
- 1144 18. Van De Leemput, I. A. *et al.* Critical slowing down as early warning for the onset and
1145 termination of depression. *Proc. Natl. Acad. Sci. U. S. A.* **111**, 87–92 (2014).
- 1146 19. Pichon, S., Miendlarzewska, E. A., Eryilmaz, H. & Vuilleumier, P. Cumulative
1147 activation during positive and negative events and state anxiety predicts subsequent
1148 inertia of amygdala reactivity. *Soc. Cogn. Affect. Neurosci.* **10**, 180–190 (2015).
- 1149 20. Suls, J., Green, P. & Hillis, S. Emotional reactivity to everyday problems, affective
1150 inertia, and neuroticism. *Personal. Soc. Psychol. Bull.* (1998).
1151 doi:10.1177/0146167298242002
- 1152 21. Koval, P., Pe, M. L., Meers, K. & Kuppens, P. Affect dynamics in relation to
1153 depressive symptoms: Variable, unstable or inert? *Emotion* **13**, 1132–1141 (2013).
- 1154 22. Trull, T. J., Lane, S. P., Koval, P. & Ebner-Priemer, U. W. Affective Dynamics in
1155 Psychopathology. *Emot. Rev.* **7**, 355–361 (2015).
- 1156 23. Lamke, J. P. *et al.* The impact of stimulus valence and emotion regulation on sustained
1157 brain activation: Task-rest switching in emotion. *PLoS One* **9**, (2014).
- 1158 24. Eryilmaz, H., Van De Ville, D., Schwartz, S. & Vuilleumier, P. Impact of transient
1159 emotions on functional connectivity during subsequent resting state: A wavelet
1160 correlation approach. *Neuroimage* **54**, 2481–2491 (2011).
- 1161 25. Pitroda, S., Angstadt, M., McCloskey, M. S., Coccaro, E. F. & Phan, K. L. Emotional
1162 experience modulates brain activity during fixation periods between tasks. *Neurosci.*
1163 *Lett.* **443**, 72–76 (2008).
- 1164 26. Waugh, C. E., Hamilton, J. P. & Gotlib, I. H. The neural temporal dynamics of the
1165 intensity of emotional experience. *Neuroimage* **49**, 1699–1707 (2010).
- 1166 27. Veer, I. M. *et al.* Beyond acute social stress: Increased functional connectivity between
1167 amygdala and cortical midline structures. *Neuroimage* **57**, 1534–1541 (2011).
- 1168 28. Eryilmaz, H., Van De Ville, D., Schwartz, S. & Vuilleumier, P. Lasting impact of
1169 regret and gratification on resting brain activity and its relation to depressive traits. *J.*
1170 *Neurosci.* **34**, 7825–7835 (2014).
- 1171 29. Waugh, C. E., Hamilton, J. P., Chen, M. C., Joormann, J. & Gotlib, I. H. Neural
1172 temporal dynamics of stress in comorbid major depressive disorder and social anxiety
1173 disorder. *Biol. Mood Anxiety Disord.* **2**, 1–15 (2012).
- 1174 30. Northoff, G., Qin, P. & Nakao, T. Rest-stimulus interaction in the brain: A review.
1175 *Trends Neurosci.* **33**, 277–284 (2010).
- 1176 31. Gavia, J., Rey, G., Bolton, T., Van De Ville, D. & Vuilleumier, P. Dynamic
1177 functional brain networks underlying the temporal inertia of negative emotions.
1178 *Neuroimage* **240**, 118377 (2021).
- 1179 32. Schneider, F. *et al.* The resting brain and our self: Self-relatedness modulates resting
1180 state neural activity in cortical midline structures. *Neuroscience* **157**, 120–131 (2008).
- 1181 33. Raichle, M. E. *et al.* A default mode of brain function. *Proc. Natl. Acad. Sci.* (2001).
1182 doi:10.1073/pnas.98.2.676
- 1183 34. Buckner, R. L., Andrews-Hanna, J. R. & Schacter, D. L. The brain's default network:
1184 Anatomy, function, and relevance to disease. *Ann. N. Y. Acad. Sci.* **1124**, 1–38 (2008).
- 1185 35. LeDoux, J. The emotional brain, fear, and the amygdala. *Cellular and Molecular*
1186 *Neurobiology* (2003). doi:10.1023/A:1025048802629

- 1187 36. Lamm, C., Decety, J. & Singer, T. Meta-analytic evidence for common and distinct
1188 neural networks associated with directly experienced pain and empathy for pain.
1189 *Neuroimage* **54**, 2492–2502 (2011).
- 1190 37. Meaux, E. & Vuilleumier, P. *Emotion Perception and Elicitation. Brain Mapping: An*
1191 *Encyclopedic Reference* **3**, (Elsevier Inc., 2015).
- 1192 38. Schuyler, B. S. *et al.* Temporal dynamics of emotional responding: Amygdala recovery
1193 predicts emotional traits. *Soc. Cogn. Affect. Neurosci.* **9**, 176–181 (2014).
- 1194 39. Kim, M. J. *et al.* The structural and functional connectivity of the amygdala: From
1195 normal emotion to pathological anxiety. *Behav. Brain Res.* **223**, 403–410 (2011).
- 1196 40. Rey, G. *et al.* Resting-state functional connectivity of emotion regulation networks in
1197 euthymic and non-euthymic bipolar disorder patients. *Eur. Psychiatry* **34**, 56–63
1198 (2016).
- 1199 41. Spreng, R. N. & Schacter, D. L. Default Network Modulation and Large-Scale
1200 Network Interactivity in Healthy Young and Old Adults. *Cereb. Cortex* **22**, 2610–2621
1201 (2012).
- 1202 42. Turner, G. R. & Spreng, R. N. Prefrontal Engagement and Reduced Default Network
1203 Suppression Co-occur and Are Dynamically Coupled in older Adults: The Default-
1204 Executive Coupling Hypothesis of Aging. *J. Cogn. Neurosci.* **27**, 2462–2476 (2015).
- 1205 43. Chen, Y.-C., Chen, C.-C., Decety, J. & Cheng, Y. Aging is associated with changes in
1206 the neural circuits underlying empathy. *Neurobiol. Aging* **35**, 827–836 (2014).
- 1207 44. Hühnel, I., Fölster, M., Werheid, K. & Hess, U. Empathic reactions of younger and
1208 older adults: No age related decline in affective responding. *J. Exp. Soc. Psychol.* **50**,
1209 136–143 (2014).
- 1210 45. Moore, R. C., Dev, S. I., Jeste, D. V., Dziobek, I. & Eyer, L. T. Distinct neural
1211 correlates of emotional and cognitive empathy in older adults. *Psychiatry Res. -*
1212 *Neuroimaging* **232**, 42–50 (2015).
- 1213 46. Tamm, S. *et al.* The effect of sleep restriction on empathy for pain: An fMRI study in
1214 younger and older adults. *Sci. Rep.* **7**, 1–14 (2017).
- 1215 47. Beadle, J. N. & De La Vega, C. E. Impact of aging on empathy: Review of
1216 psychological and neural mechanisms. *Front. Psychiatry* **10**, 1–13 (2019).
- 1217 48. Sze, J. A., Gyurak, A., Goodkind, M. S. & Levenson, R. W. Greater emotional
1218 empathy and prosocial behavior in late life. *Emotion* **12**, 1129–1140 (2012).
- 1219 49. Bailey, P. E., Brady, B., Ebner, N. C. & Ruffman, T. Effects of age on emotion
1220 regulation, emotional empathy, and prosocial behavior. *Journals Gerontol. - Ser. B*
1221 *Psychol. Sci. Soc. Sci.* **75**, 802–810 (2020).
- 1222 50. Fan, Y., Duncan, N. W., de Greck, M. & Northoff, G. Is there a core neural network in
1223 empathy? An fMRI based quantitative meta-analysis. *Neurosci. Biobehav. Rev.* **35**,
1224 903–911 (2011).
- 1225 51. Schurz, M., Radua, J., Aichhorn, M., Richlan, F. & Perner, J. Fractionating theory of
1226 mind: A meta-analysis of functional brain imaging studies. *Neurosci. Biobehav. Rev.*
1227 **42**, 9–34 (2014).
- 1228 52. Krueger, K. R. *et al.* Social engagement and cognitive function in old age. *Exp. Aging*
1229 *Res.* **35**, 45–60 (2009).
- 1230 53. MacLeod, S., Musich, S., Hawkins, K., Alsgaard, K. & Wicker, E. R. The impact of
1231 resilience among older adults. *Geriatr. Nurs. (Minneap)*. **37**, 266–272 (2016).
- 1232 54. Zunzunegui, M. V., Alvarado, B. E., Del Ser, T. & Otero, A. Social networks, social
1233 integration, and social engagement determine cognitive decline in community-dwelling
1234 Spanish older adults. *Journals Gerontol. - Ser. B Psychol. Sci. Soc. Sci.* **58**, (2003).
- 1235 55. Klimecki, O. M., Leiberg, S., Lamm, C. & Singer, T. Functional neural plasticity and
1236 associated changes in positive affect after compassion training. *Cereb. Cortex* **23**,

- 1237 1552–1561 (2013).
- 1238 56. Gross, J. J. The emerging field of emotion regulation: An integrative review. *Review of*
1239 *General Psychology* (1998). doi:10.1037/1089-2680.2.3.271
- 1240 57. Poinsel, G. *et al.* The Age-Well randomized controlled trial of the Medit-Ageing
1241 European project: Effect of meditation or foreign language training on brain and mental
1242 health in older adults. *Alzheimer's Dement. Transl. Res. Clin. Interv.* **4**, 714–723
1243 (2018).
- 1244 58. Davis, M. H. & Association, A. P. A multidimensional approach to individual
1245 differences in empathy. *JSAS Cat. Sel. Doc. Psychol.* (1980).
- 1246 59. Sheikh, J. I. & Yesavage, J. A. 9/geriatric depression scale (Gds) recent evidence and
1247 development of a shorter version. *Clin. Gerontol.* (1986). doi:10.1300/J018v05n01_09
- 1248 60. Beck, A. T., Steer, R. A., & Brown, G. K. (1996). BDI-II manual. San Antonio, TX:
1249 The Psychological Corporation.
- 1250 61. Spielberger, C. D., Gorsuch, R. L. & Lushene, R. State-trait anxiety inventory STAI
1251 (Form Y). *Redw. City Mind Gard.* (1983). doi:10.1515/9783111677439-035
- 1252 62. Gross, J. J. & John, O. P. Individual differences in two emotion regulation processes:
1253 Implications for affect, relationships, and well-being. *J. Pers. Soc. Psychol.* **85**, 348–
1254 362 (2003).
- 1255 63. Treynore, Gonzalez & Nolen-Hoeksema, S. Ruminative Responses Scale. *Cognit.*
1256 *Ther. Res.* (2003). doi:10.1017/CBO9781107415324.004
- 1257 64. Klimecki, O. M., Leiberg, S., Ricard, M. & Singer, T. Differential pattern of functional
1258 brain plasticity after compassion and empathy training. *Soc. Cogn. Affect. Neurosci.* **9**,
1259 873–879 (2013).
- 1260 65. Taylor, W. D. *et al.* Smaller orbital frontal cortex volumes associated with functional
1261 disability in depressed elders. *Biol. Psychiatry* **53**, 144–149 (2003).
- 1262 66. Grimm, S. *et al.* Segregated neural representation of distinct emotion dimensions in the
1263 prefrontal cortex - An fMRI study. *Neuroimage* **30**, 325–340 (2006).
- 1264 67. Benjamini, Y. & Hochberg, Y. Controlling the False Discovery Rate: A Practical and
1265 Powerful Approach to Multiple Testing. *J. R. Stat. Soc. Ser. B* (1995).
1266 doi:10.1111/j.2517-6161.1995.tb02031.x
- 1267 68. Pruim, R. H. R. *et al.* ICA-AROMA: A robust ICA-based strategy for removing motion
1268 artifacts from fMRI data. *Neuroimage* **112**, 267–277 (2015).
- 1269 69. Villain, N. *et al.* A simple way to improve anatomical mapping of functional brain
1270 imaging. *J. Neuroimaging* **20**, 324–333 (2010).
- 1271 70. Power, J. D., Barnes, K. A., Snyder, A. Z., Schlaggar, B. L. & Petersen, S. E. Spurious
1272 but systematic correlations in functional connectivity MRI networks arise from subject
1273 motion. *Neuroimage* **59**, 2142–2154 (2012).
- 1274 71. Lieberman, M. D. & Cunningham, W. A. Type I and Type II error concerns in fMRI
1275 research: Re-balancing the scale. *Soc. Cogn. Affect. Neurosci.* **4**, 423–428 (2009).
- 1276 72. Andrews-Hanna, J. R., Reidler, J. S., Sepulcre, J., Poulin, R. & Buckner, R. L.
1277 Functional-Anatomic Fractionation of the Brain's Default Network. *Neuron* **65**, 550–
1278 562 (2010).
- 1279 73. Fair, D. A. *et al.* A method for using blocked and event-related fMRI data to study
1280 'resting state' functional connectivity. *Neuroimage* **35**, 396–405 (2007).
- 1281 74. Friston, K. J. Functional and effective connectivity in neuroimaging: A synthesis. *Hum.*
1282 *Brain Mapp.* **2**, 56–78 (1994).
- 1283 75. Winkler, A. M., Ridgway, G. R., Webster, M. A., Smith, S. M. & Nichols, T. E.
1284 Permutation inference for the general linear model. *Neuroimage* **92**, 381–397 (2014).
- 1285 76. Wancata, J., Alexandrowicz, R., Marquart, B., Weiss, M. & Friedrich, F. The criterion
1286 validity of the geriatric depression scale: A systematic review. *Acta Psychiatr. Scand.*

- 1287 **114**, 398–410 (2006).
- 1288 77. Singer, T. & Klimecki, O. M. Empathy and compassion. *Curr. Biol.* **24**, R875–R878
1289 (2014).
- 1290 78. Corradi-Dell’Acqua, C., Hofstetter, C. & Vuilleumier, P. Cognitive and affective
1291 theory of mind share the same local patterns of activity in posterior temporal but not
1292 medial prefrontal cortex. *Soc. Cogn. Affect. Neurosci.* **9**, 1175–1184 (2014).
- 1293 79. Preckel, K., Kanske, P. & Singer, T. On the interaction of social affect and cognition:
1294 empathy, compassion and theory of mind. *Curr. Opin. Behav. Sci.* **19**, 1–6 (2018).
- 1295 80. Klimecki, O. M. *et al.* The impact of meditation on healthy ageing — the current state
1296 of knowledge and a roadmap to future directions. *Curr. Opin. Psychol.* **28**, 223–228
1297 (2019).
- 1298 81. Cacioppo, J. T. & Berntson, G. G. Relationship Between Attitudes and Evaluative
1299 Space: A Critical Review, With Emphasis on the Separability of Positive and Negative
1300 Substrates. *Psychol. Bull.* **115**, 401–423 (1994).
- 1301 82. Norman, G. J. *et al.* Current emotion research in psychophysiology: The neurobiology
1302 of evaluative bivalence. *Emot. Rev.* **3**, 349–359 (2011).
- 1303 83. Seeley, W. W. *et al.* Dissociable intrinsic connectivity networks for salience processing
1304 and executive control. *J. Neurosci.* **27**, 2349–2356 (2007).
- 1305 84. Menon, V. & Uddin, L. Q. Saliency, switching, attention and control: a network model
1306 of insula function. *Brain Struct. Funct.* **214**, 655–667 (2010).
- 1307 85. Knutson, B., Katovich, K. & Suri, G. Inferring affect from fMRI data. *Trends Cogn.*
1308 *Sci.* **18**, 422–428 (2014).
- 1309 86. Corradi-Dell’Acqua, C., Tusche, A., Vuilleumier, P. & Singer, T. Cross-modal
1310 representations of first-hand and vicarious pain, disgust and fairness in insular and
1311 cingulate cortex. *Nat. Commun.* **7**, (2016).
- 1312 87. Bruneau, E. G., Jacoby, N. & Saxe, R. Empathic control through coordinated
1313 interaction of amygdala, theory of mind and extended pain matrix brain regions.
1314 *Neuroimage* **114**, 105–119 (2015).
- 1315 88. Bruneau, E., Dufour, N. & Saxe, R. How We Know It Hurts: Item Analysis of Written
1316 Narratives Reveals Distinct Neural Responses to Others’ Physical Pain and Emotional
1317 Suffering. *PLoS One* **8**, (2013).
- 1318 89. Knutson, B., Fong, G. W., Adams, C. M., Varner, J. L. & Hommer, D. Dissociation of
1319 reward anticipation and outcome with event-related fMRI. *Neuroreport* **12**, 3683–3687
1320 (2001).
- 1321 90. Sander, D., Grafman, J. & Zalla, T. The Human Amygdala: An Evolved System for
1322 Relevance Detection. *Reviews in the Neurosciences* (2003).
1323 doi:10.1515/REVNEURO.2003.14.4.303
- 1324 91. Cunningham, W. A., Raye, C. L. & Johnson, M. K. 0898929042947919. 1–13 (2004).
- 1325 92. Riva, F. *et al.* Age-related differences in the neural correlates of empathy for pleasant
1326 and unpleasant touch in a female sample. *Neurobiol. Aging* **65**, 7–17 (2018).
- 1327 93. Dolcos, S., Moore, M. & Katsumi, Y. Neuroscience and Well-Being. 1–26 (2018).
- 1328 94. Davidson, R. J. Affective Style and Affective Disorders: Perspectives from Affective
1329 Neuroscience. *Cogn. Emot.* **12**, 307–330 (1998).
- 1330 95. Davidson, R. J. Well-being and affective style: Neural substrates and biobehavioural
1331 correlates. *Philos. Trans. R. Soc. B Biol. Sci.* **359**, 1395–1411 (2004).
- 1332 96. Koval, P., Butler, E. A., Hollenstein, T., Lanteigne, D. & Kuppens, P. Emotion
1333 regulation and the temporal dynamics of emotions: Effects of cognitive reappraisal and
1334 expressive suppression on emotional inertia. *Cogn. Emot.* **29**, 831–851 (2015).
- 1335 97. Lamm, C. & Singer, T. The role of anterior insular cortex in social emotions. *Brain*
1336 *Struct. Funct.* **214**, 579–591 (2010).

- 1337 98. Makovac, E., Fagioli, S., Rae, C. L., Critchley, H. D. & Ottaviani, C. Can't get it off
1338 my brain: Meta-analysis of neuroimaging studies on perseverative cognition.
1339 *Psychiatry Res. - Neuroimaging* **295**, 111020 (2020).
- 1340 99. Addis, D. R., Wong, A. T. & Schacter, D. L. Remembering the past and imagining the
1341 future: Common and distinct neural substrates during event construction and
1342 elaboration. *Neuropsychologia* **45**, 1363–1377 (2007).
- 1343 100. Mason, M. F. *et al.* Wandering minds: The default network and stimulus-independent
1344 thought. *Science (80-.)*. **315**, 393–395 (2007).
- 1345 101. Phelps, E. A. & LeDoux, J. E. Contributions of the amygdala to emotion processing:
1346 From animal models to human behavior. *Neuron* **48**, 175–187 (2005).
- 1347 102. Ehring, T. & Watkins, E. R. Repetitive Negative Thinking as a Transdiagnostic
1348 Process. *Int. J. Cogn. Ther.* **1**, 192–205 (2008).
- 1349 103. Jagust, W. Imaging the evolution and pathophysiology of Alzheimer disease. *Nat. Rev.*
1350 *Neurosci.* (2018). doi:10.1038/s41583-018-0067-3
- 1351 104. Leech, R. & Sharp, D. J. The role of the posterior cingulate cortex in cognition and
1352 disease. *Brain* **137**, 12–32 (2014).
- 1353 105. Critchley, H. D., Wiens, S., Rotshtein, P., Öhman, A. & Dolan, R. J. Neural systems
1354 supporting interoceptive awareness. *Nat. Neurosci.* **7**, 189–195 (2004).
- 1355 106. Zaki, J., Davis, J. I. & Ochsner, K. N. Overlapping activity in anterior insula during
1356 interoception and emotional experience. *Neuroimage* **62**, 493–499 (2012).
- 1357 107. Amodio, D. M. & Frith, C. D. Meeting of minds: The medial frontal cortex and social
1358 cognition. *Nature Reviews Neuroscience* **7**, 268–277 (2006).
- 1359 108. Juchem, C., Nixon, T. W., McIntyre, S., Rothman, D. L. & De Graaf, R. A. Magnetic
1360 field homogenization of the human prefrontal cortex with a set of localized electrical
1361 coils. *Magn. Reson. Med.* **63**, 171–180 (2010).
- 1362

1363 ACKNOWLEDGMENTS

1364
1365
1366
1367
1368
1369
1370
1371
1372
1373
1374
1375
1376
1377
1378
1379
1380

The Age-Well randomized clinical trial is part of the Medit-Ageing project and is funded through the European Union’s Horizon 2020 Research and Innovation Program (grant agreement n°667696), Institut National de la Santé et de la Recherche Médicale, Région Normandie, and Fondation d’Entreprise MMA des Entrepreneurs du Futur. Institut National de la Santé et de la Recherche Médicale (Inserm) is the sponsor. The funders and sponsor had no role in the design and conduct of the study, collection, management, analysis, and interpretation of the data, preparation, review, or approval of the manuscript, and decision to submit the manuscript for publication. The authors are grateful to the Cyceron staff members for their help with neuroimaging data acquisition; as well as to the EUCLID team, the sponsor (Hélène Espérou – Pôle de recherche Clinique Inserm) and to all the participants in this study for their contribution. We acknowledge and thank the Medit-Ageing Research Group members for their contribution. We thank Clara Bordas, Silvia de Cataldo, and Julia Sachs for their help on the mental thoughts analyses and their dedication during data acquisition. We also thank Bruno Bonnet and Frédéric Grouiller as the principal staff members of the Brain and Behavior Laboratory in Geneva.

1381 AUTHOR CONTRIBUTIONS

1382
1383
1384
1385
1386
1387
1388

1389
1390

Conceptualization: S.B.L., O.K., and P.V.; Data curation: S.B.L., Y.I.D.A., C.M., O.K., and P.V.; Formal analysis: S.B.L., and Y.I.D.A.; Funding acquisition: O.K., N.L.M, G.C., and P.V.; Investigation: S.B.L., C.M., and members of the Medit-Ageing Research Group; Methodology: S.B.L., Y.I.D.A., O.K., G.C., and P.V.; Supervision: O.K., and P.V.; Visualization: S.B.L.; Writing – Original Draft: S.B.L.; Writing – Review and Editing: S.B.L., F.C., G.C., N.L.M., O.K., P.V., C.M., and Y.I.D.A.

1391 **COMPETING INTERESTS**

1392
 1393 Dr. Chételat reported personal fees from Fondation Entrepreneurs MMA and from Fondation
 1394 Alzheimer. No other disclosures were reported.

1395
 1396
 1397
 1398
 1399

MEDIT-AGEING RESEARCH GROUP MEMBERS

SURNAME	FORENAME	EMAIL ADDRESS
Arenaza Urquijo	Eider	eiderarenaza@gmail.com
André	Claire	andré@cyceron.fr
Baez Lugo	Sebastian	sebastian.baezlugo@unige.ch
Botton	Maelle	botton@cyceron.fr
Cantou	Pauline	Cantou@cyceron.fr
Chételat	Gaëlle	chetelat@cyceron.fr
Chocat	Anne	annechocat@orange.fr
Collette	Fabienne	f.collette@uliege.be
De la Sayette	Vincent	delasayette-v@chu-caen.fr
Delarue	Marion	delarue@cyceron.fr
Egret	Stéphanie	egret@cyceron.fr
Ferrand Devouge	Eglantine	eglantine.ferranddevouge@gmail.com
Frison	Eric	Eric.Frison@isped.u-bordeaux2.fr
Gonneaud	Julie	gonneaud@cyceron.fr
Heidmann	Marc	marc.heidmann@ens-lyon.fr
Klimecki	Olga	Olga.Klimecki@unige.ch
Kuhn	Elizabeth	kuhn@cyceron.fr
Landeau	Brigitte	landeau@cyceron.fr
Le Du	Gwendoline	ledu@cyceron.fr
Lefranc	Valérie	lefranc@cyceron.fr
Lutz	Antoine	antoine.lutz@inserm.fr
Marchant	Natalie	n.marchant@ucl.ac.uk
Mezenge	Florence	mezenge@cyceron.fr
Moulinet	Inès	moulinet@cyceron.fr
Ourry	Valentin	ourry@cyceron.fr
Poisnel	Géraldine	poisnel@cyceron.fr
Quillard	Anne	anne.quillard@ch-flers.fr
Rauchs	Géraldine	rauchs@cyceron.fr
Rehel	Stéphane	rehel@cyceron.fr
Tomadesso	Clémence	tomadesso@cyceron.fr
Touron	Edelweiss	touron@cyceron.fr
Vuilleumier	Patrik	patrik.vuilleumier@unige.ch
Ware	Caitlin	caitlin.ware@gmail.com
Wirth	Miranka	miranka.wirth@charite.de

1400